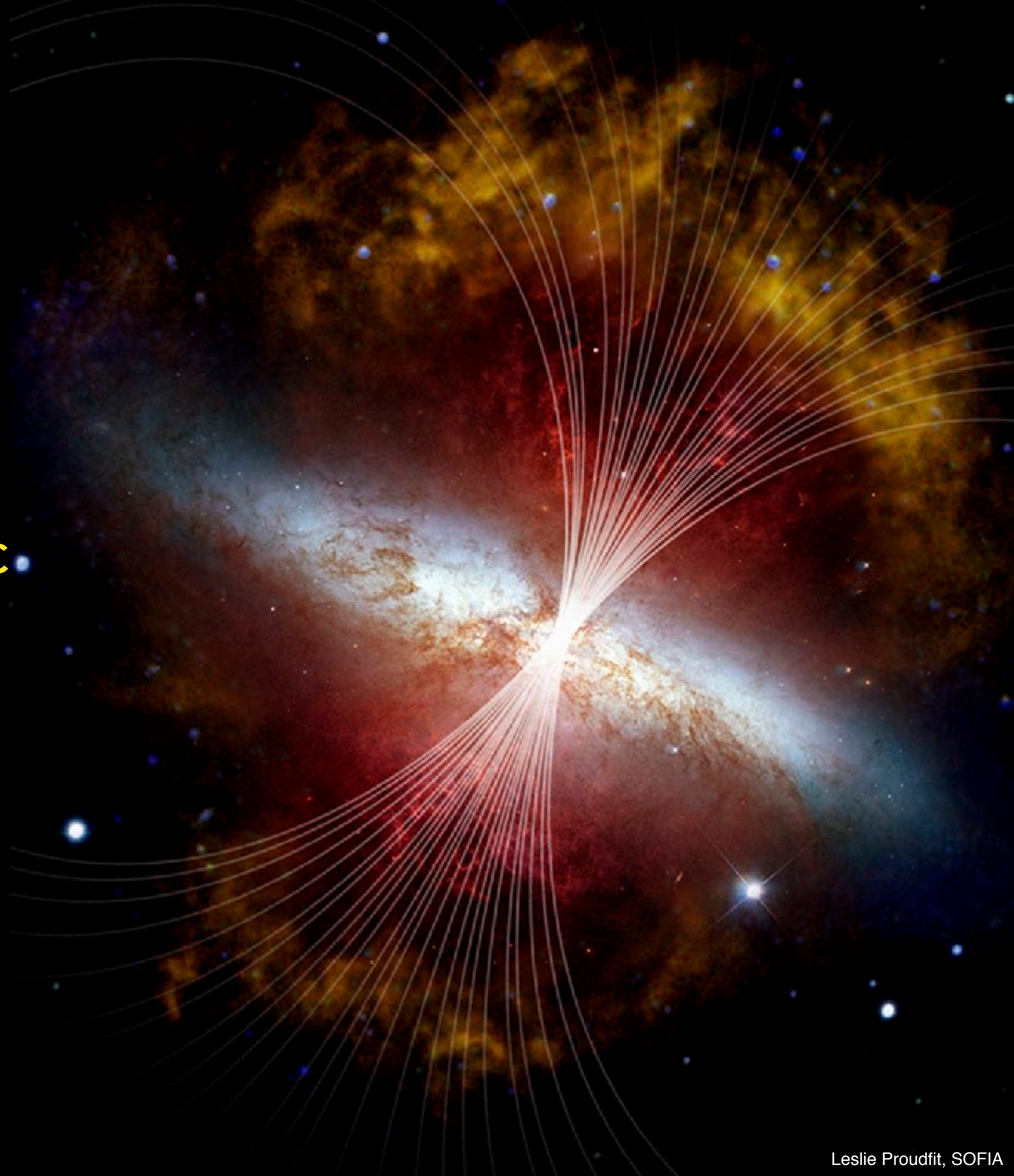


THE STRENGTH AND STRUCTURE OF THE MAGNETIC FIELD IN THE GALACTIC OUTFLOW OF M82

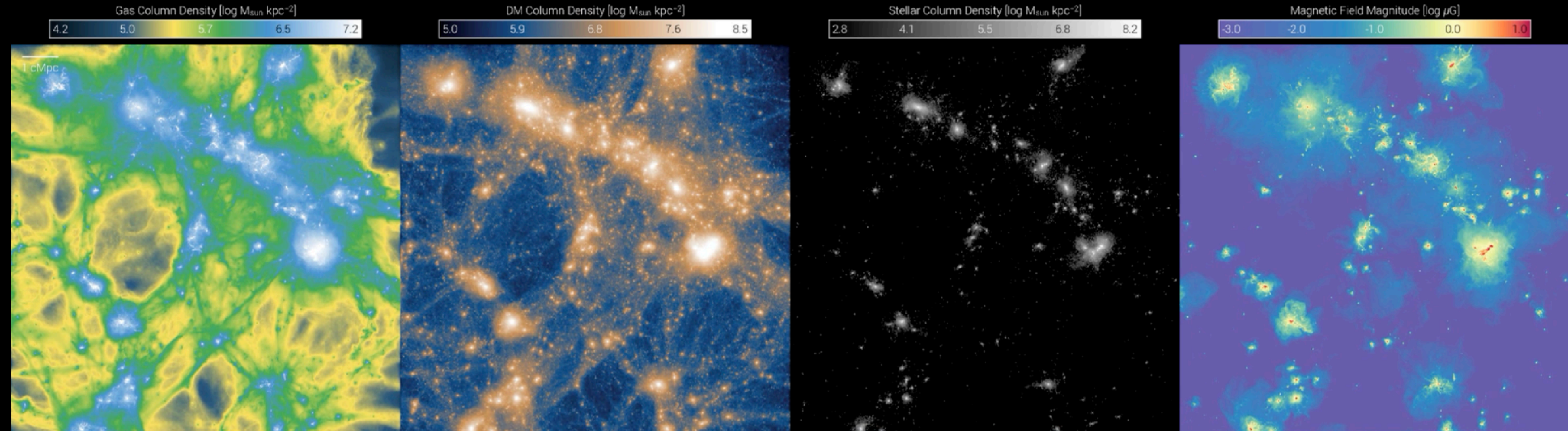
Enrique Lopez Rodriguez, Jordan A. Guerra, Mah Asgari-Targhi, Joan Schmelz

Kavli Institute for Particle Astrophysics and Cosmology (KIPAC)
Stanford University



THE ROLE OF MAGNETIC FIELDS IN GALAXY EVOLUTION

Magnetic fields are amplified as a consequence of galaxy formation and turbulence-driven dynamos.



Stage 1: Field seeds

- Generation of seed fields by Biermann battery, Weibel instability, or plasma fluctuations ($B \sim 10^{-18} - 10^{-6}$ G).

Stage 2: Field Amplification

- Amplification of seed fields by turbulent gas flows, i.e. small-scale dynamo ($B \sim 10^{-5}$ G).
- Turbulence is driven by accretion flows and SN explosions.

Stage 3: Field ordering

- Field ordered (stretched) by shear and by large-scale dynamo ($t \sim 10^9$ yr).
- Turbulence driven by SN explosions and magnetorotational instability (MRI) in galaxy disks.

THE ROLE OF STARBURST IN GALAXY EVOLUTION: M82 AS CANONICAL EXAMPLE

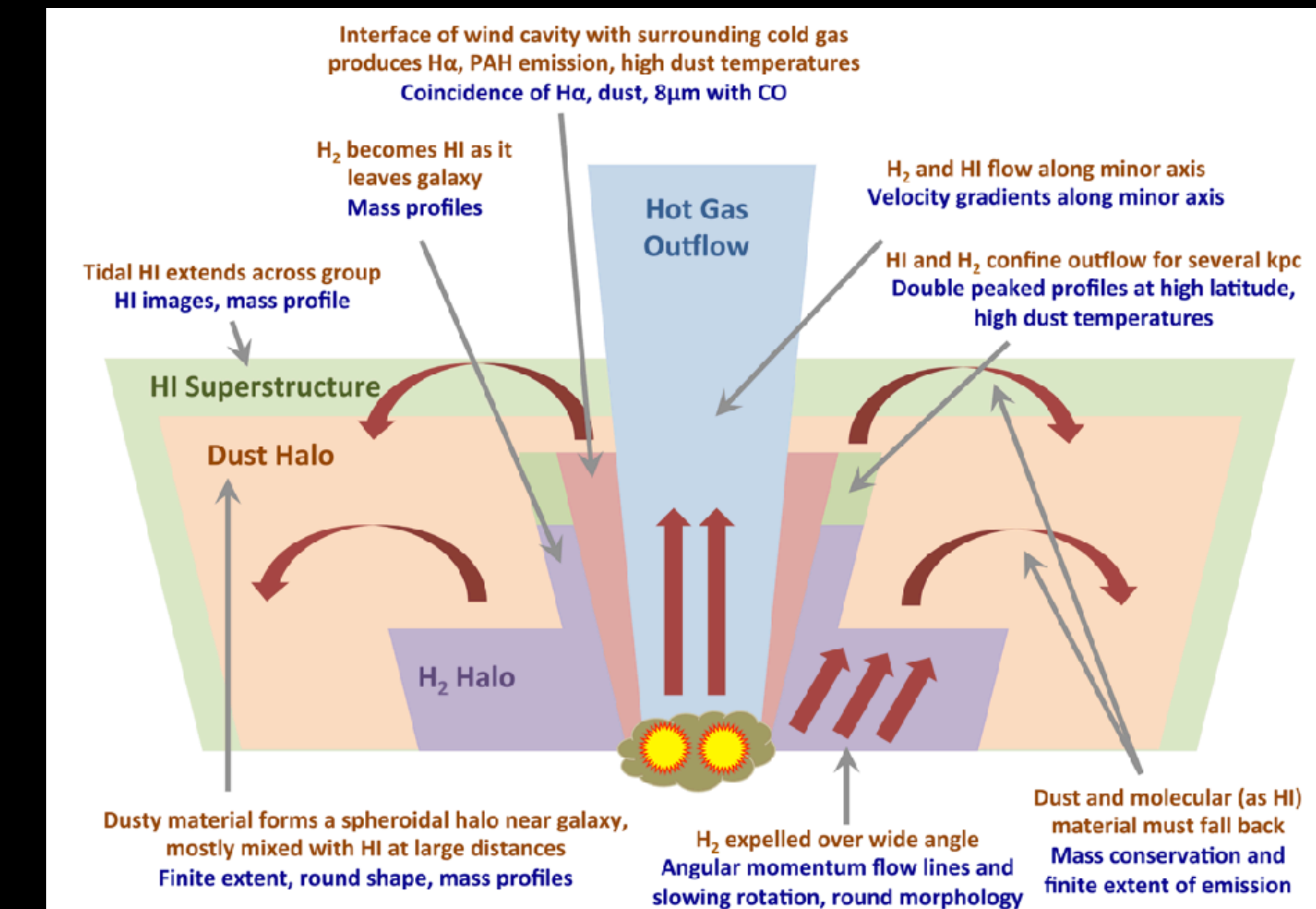
'Galactic winds are the primary mechanism by which energy and metals are recycle in galaxies and deposited into the IGM'

Veilleux, Cecil & Bland-Hawthorn's ARAA Review (2005)

D = 3.85 Mpc (20 pc/", Vacca et al. 2015)

Bipolar superwind driven by extreme star formation regions.

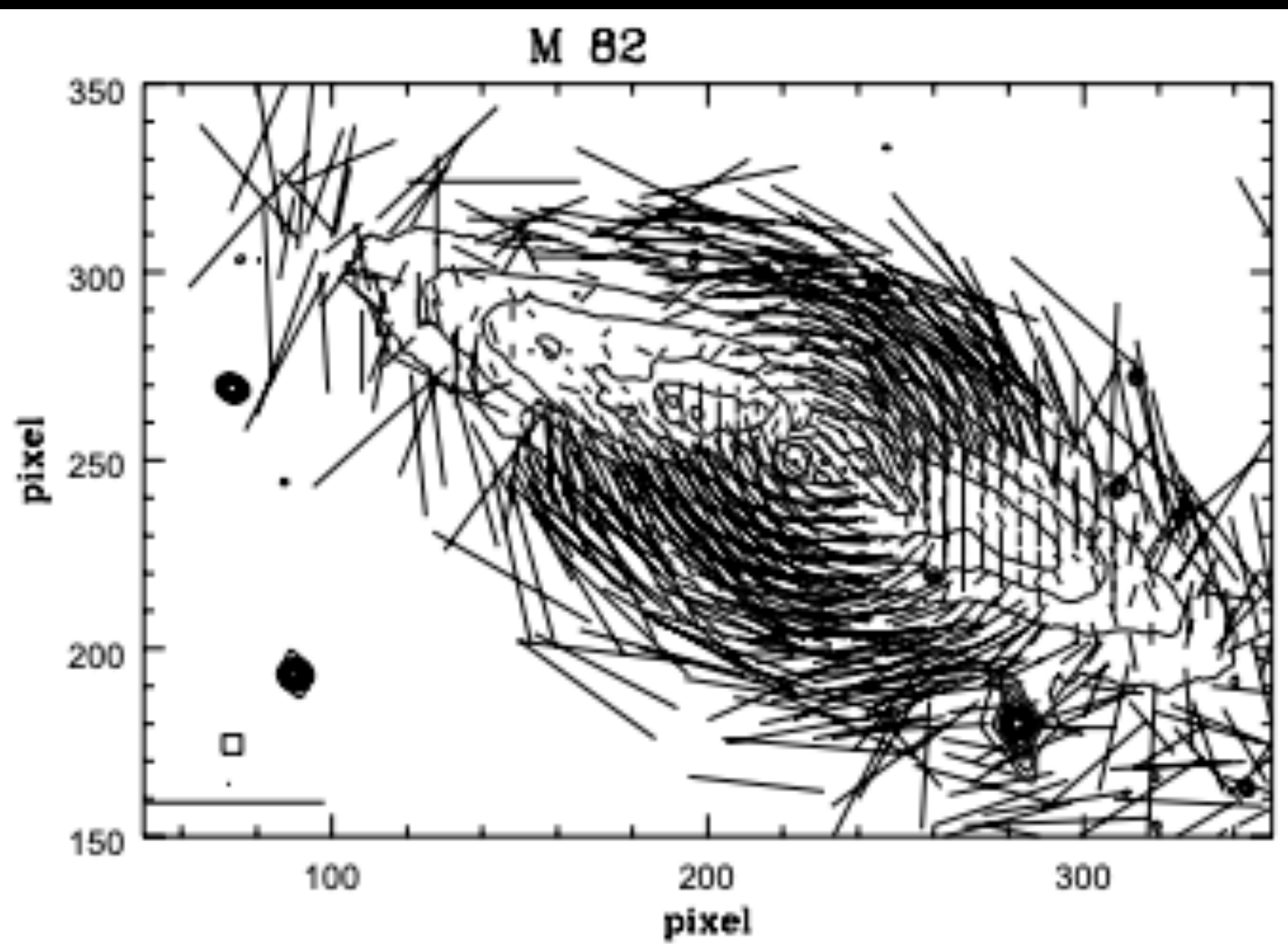
Galactic wind is extended and perpendicular to the galactic plane up to ~10 kpc.



Credit: NASA

Leroy et al. (2015)

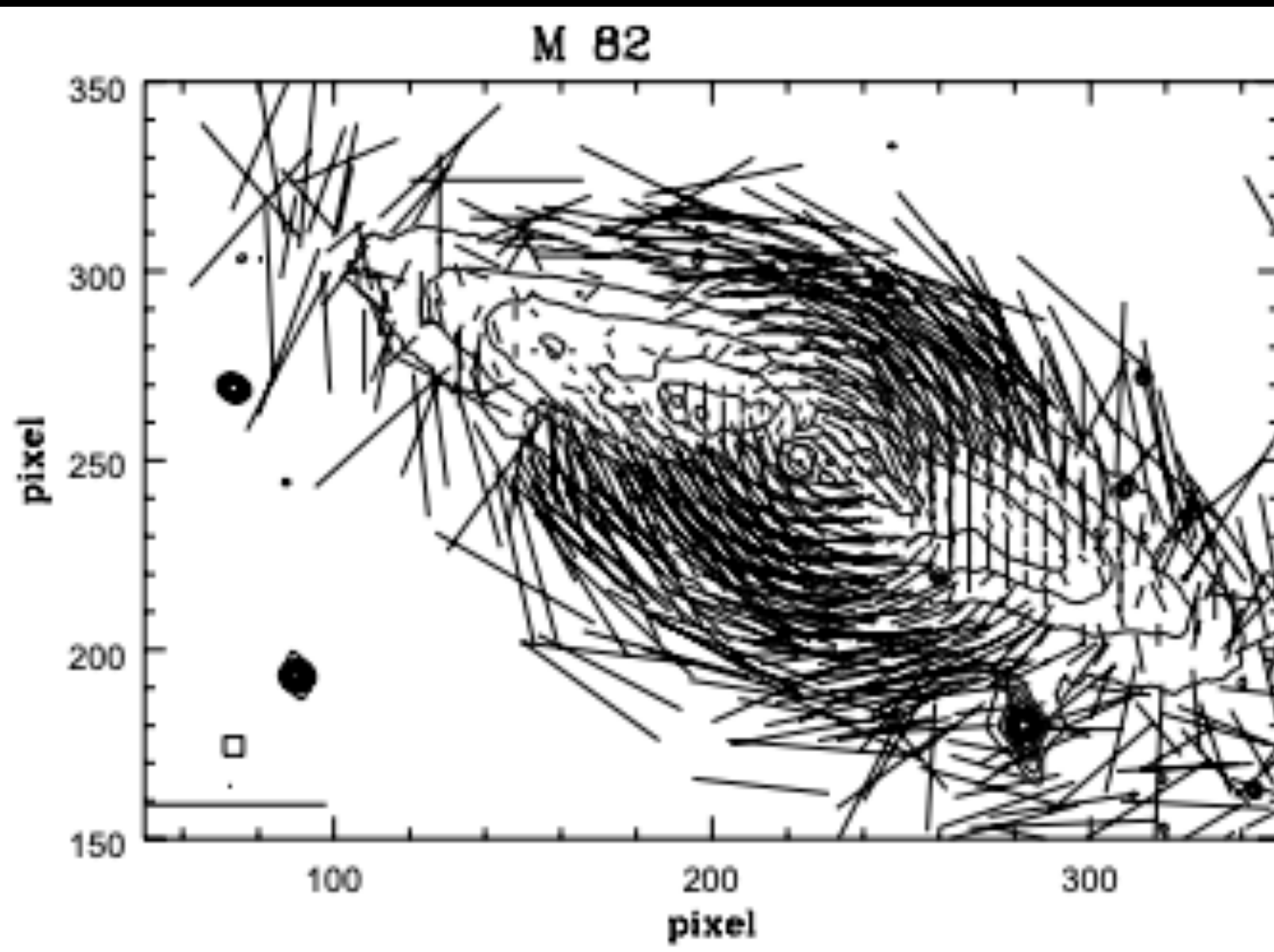
MAGNETIC FIELDS IN M82: OPTICAL



Optical (R-band, 0.65 μ m)
Polarization dominated by dust scattering.
Centrosymmetric pattern in the starburst region.
No information about B-fields.

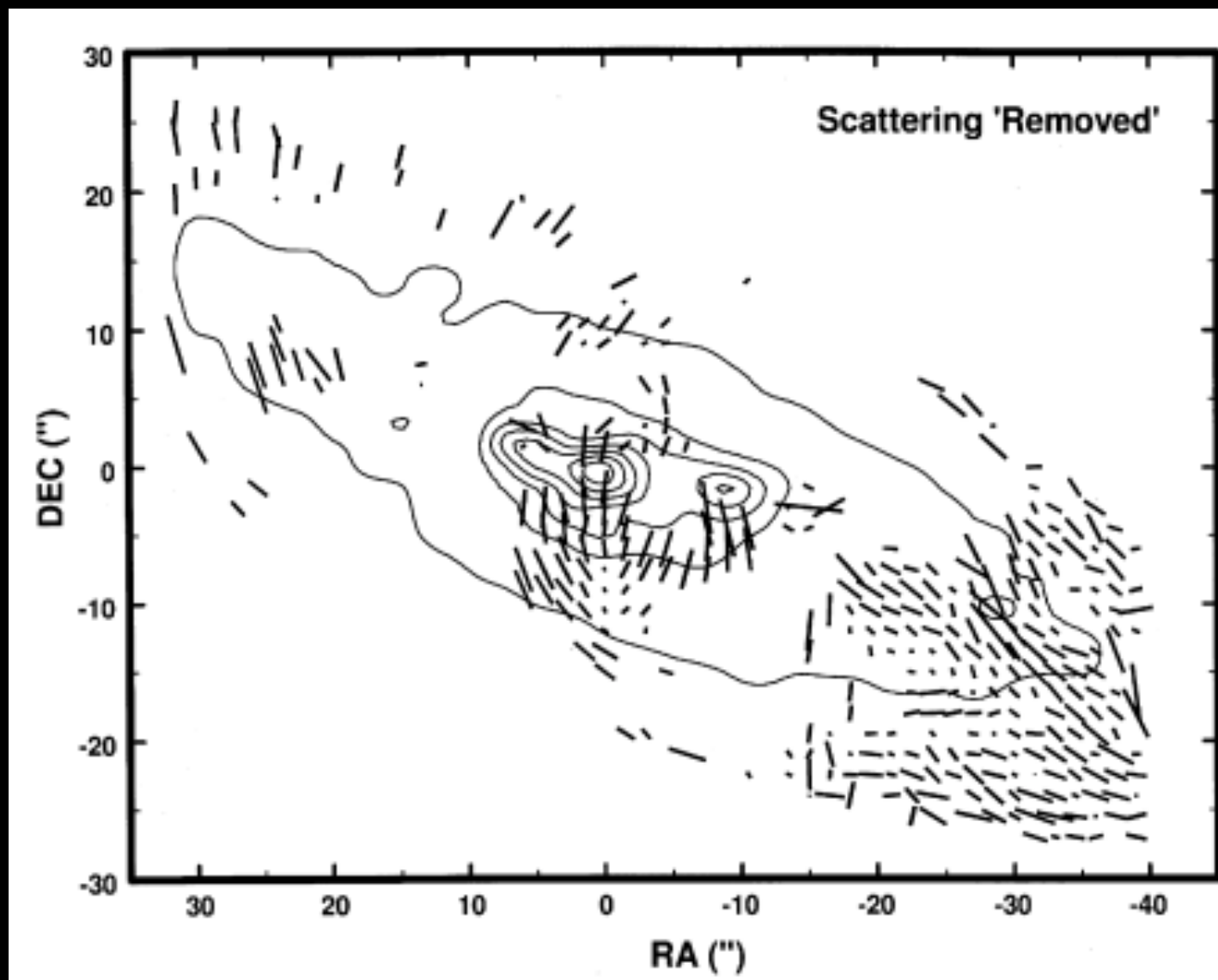
Fendt, Beck, Neininger (1998)

MAGNETIC FIELDS IN M82: NEAR-INFRARED



Optical (R-band, $0.65 \mu\text{m}$)
Polarization dominated by dust scattering.
Centrosymmetric pattern in the starburst region.
No information about B-fields.

Fendt, Beck, Neininger (1998)



Near-Infrared (H-band, $1.65 \mu\text{m}$)
Dust scattering has been removed.
Hints of:

- Vertical B-field in the core
- B-field along the galactic plane

Polarization mechanism:

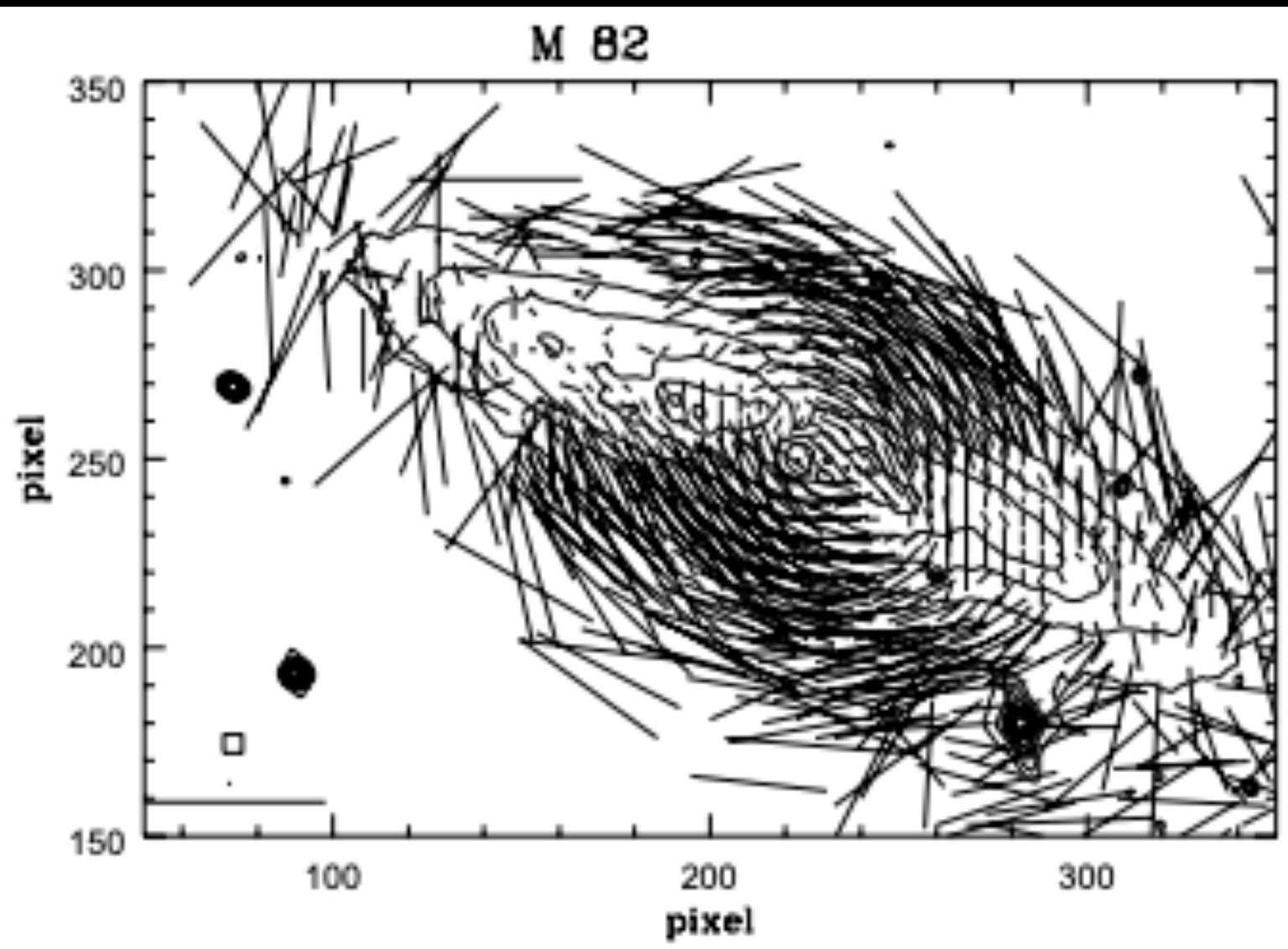
- Magnetically aligned dust grains (dichroic absorption)

B-fields are:

1. Along the galactic plane (galactic dynamo)
2. Along the galactic wind (galactic outflow)

Jones (2000)

MAGNETIC FIELDS IN M82: RADIO

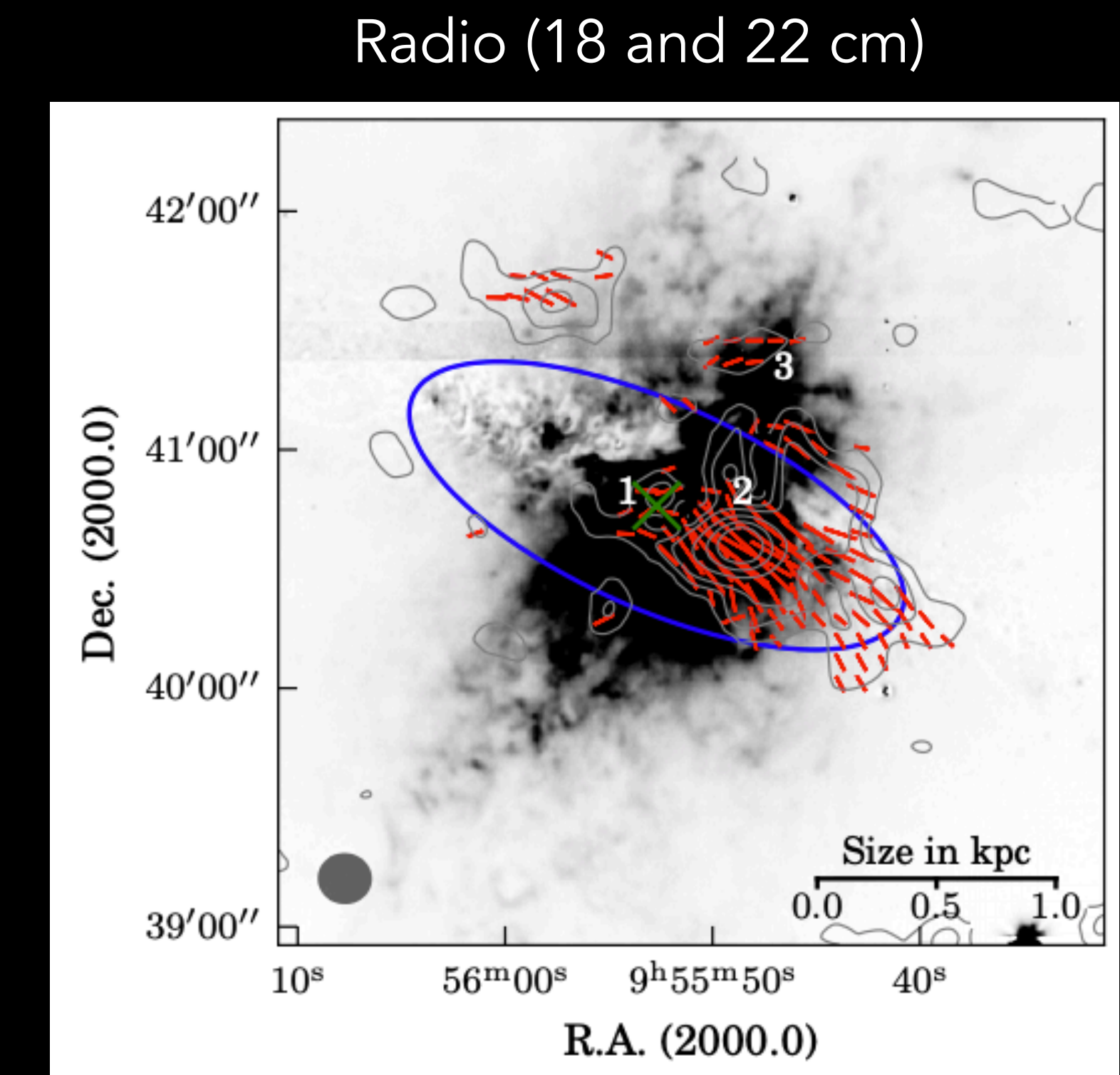


Optical (R-band, 0.65 μm)

Polarization dominated by dust scattering.

Centrosymmetric pattern in the starburst region.

No information about B-fields.



Adeahr et al. (2017)

Near-Infrared (H-band, 1.65 μm)

Dust scattering has been removed.

Hints of:

- Vertical B-field in the core
- B-field along the galactic plane

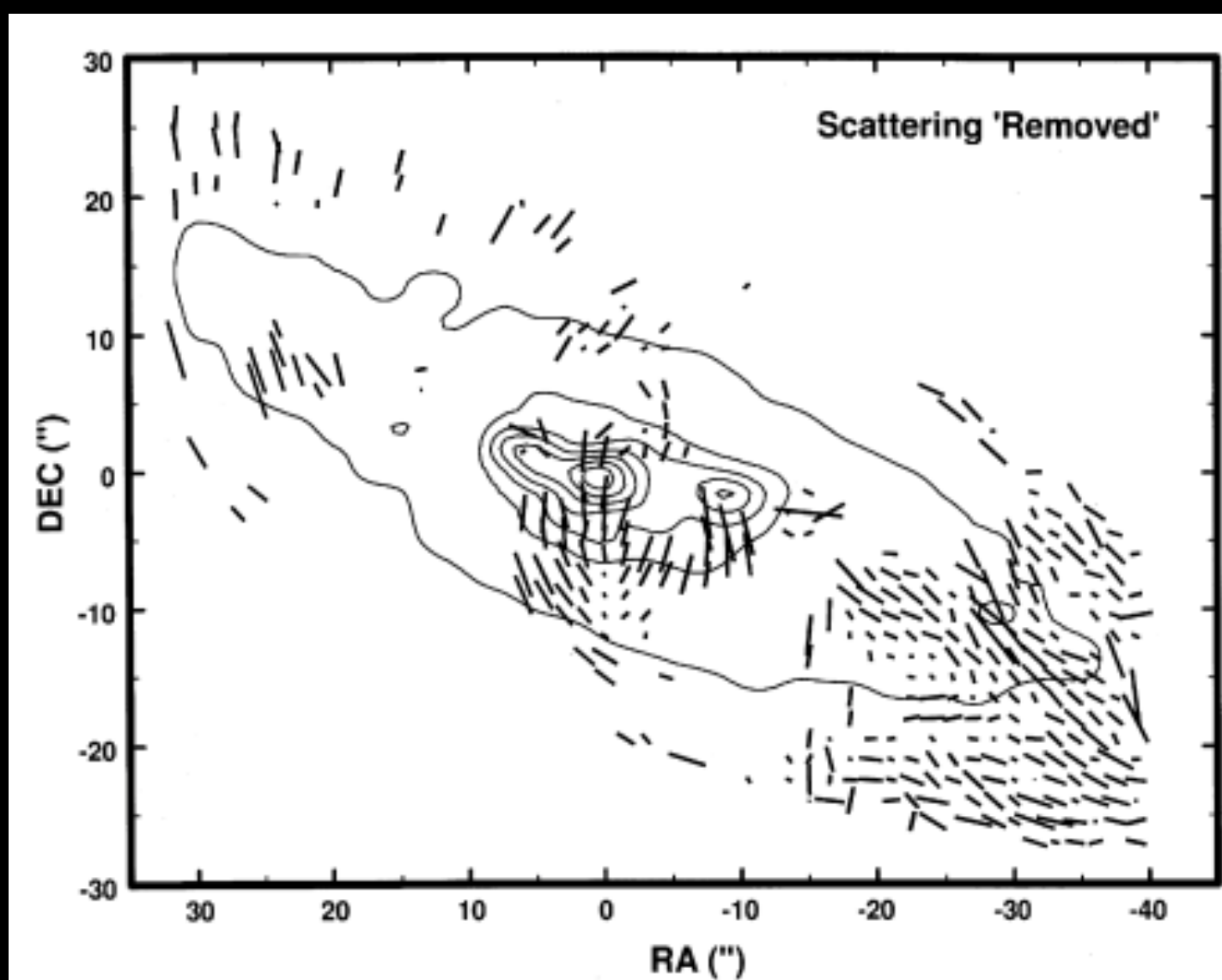
Polarization mechanism:

- Magnetically aligned dust grains (dichroic absorption)

B-fields are:

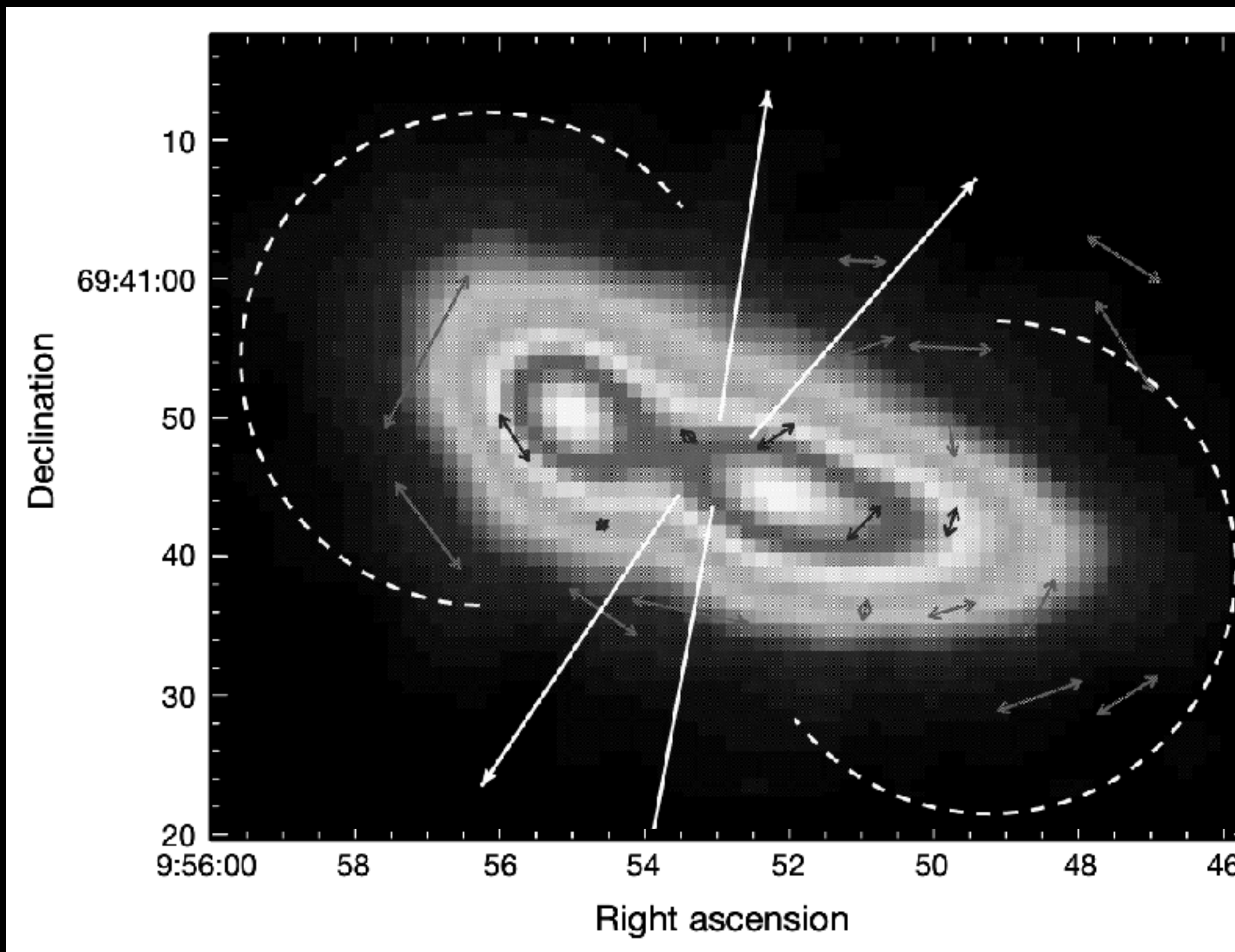
1. Along the galactic plane (galactic dynamo)
2. Along the galactic wind (galactic outflow)

Jones (2000)



MAGNETIC FIELDS IN M82: SUB-MM

Sub-mm (850 μ m, SCUPOL/JCMT)
Same dataset reduced independently.

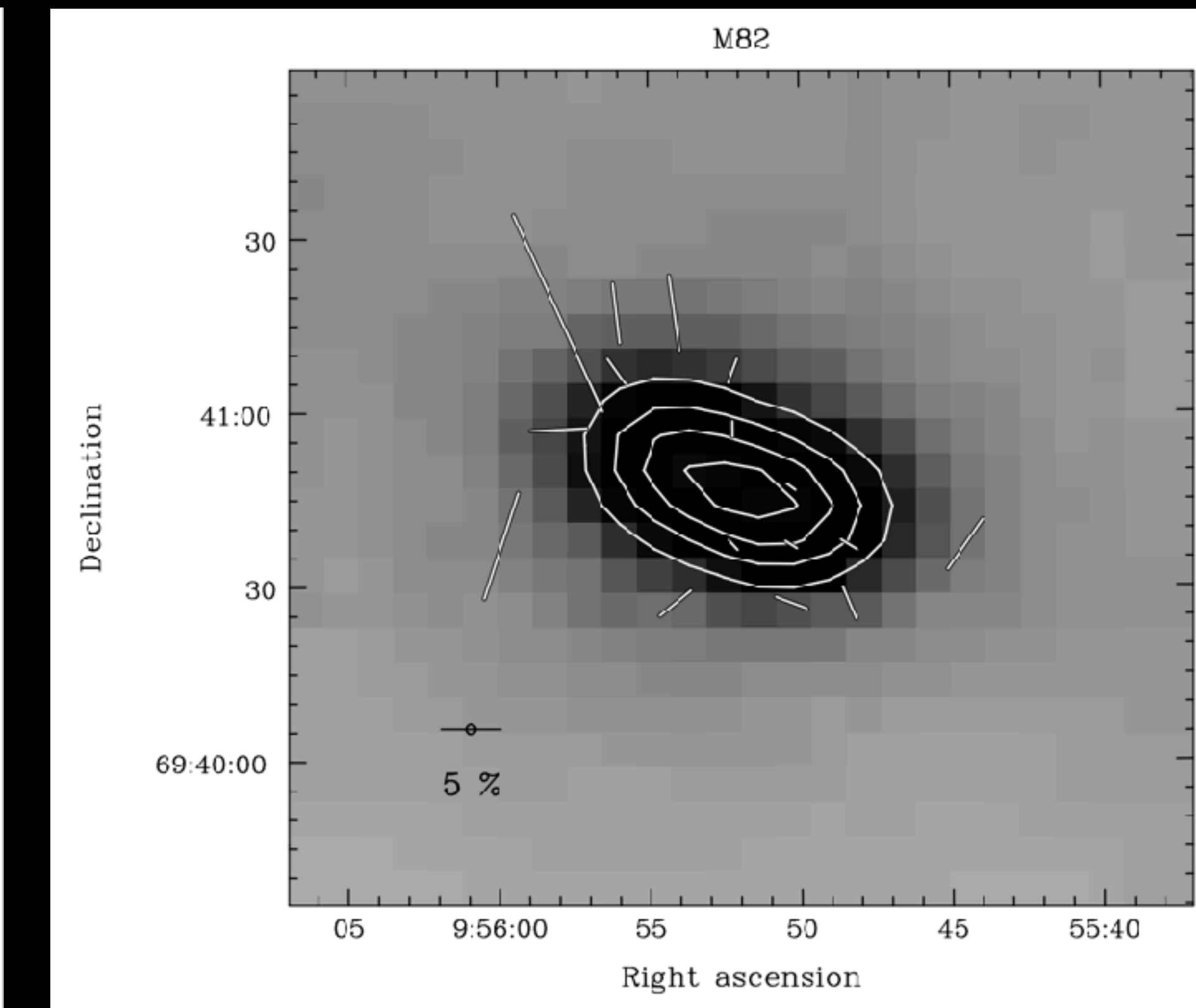


Greaves et al. (2000) Greaves et al. (2002)

Polarization dominated by magnetically aligned dust grains.
Potential 'giant magnetic bubble'.

colorscale: 450 μ m

Black lines above 50% flux level.
 $P > 3\sigma$ at 12" resolution



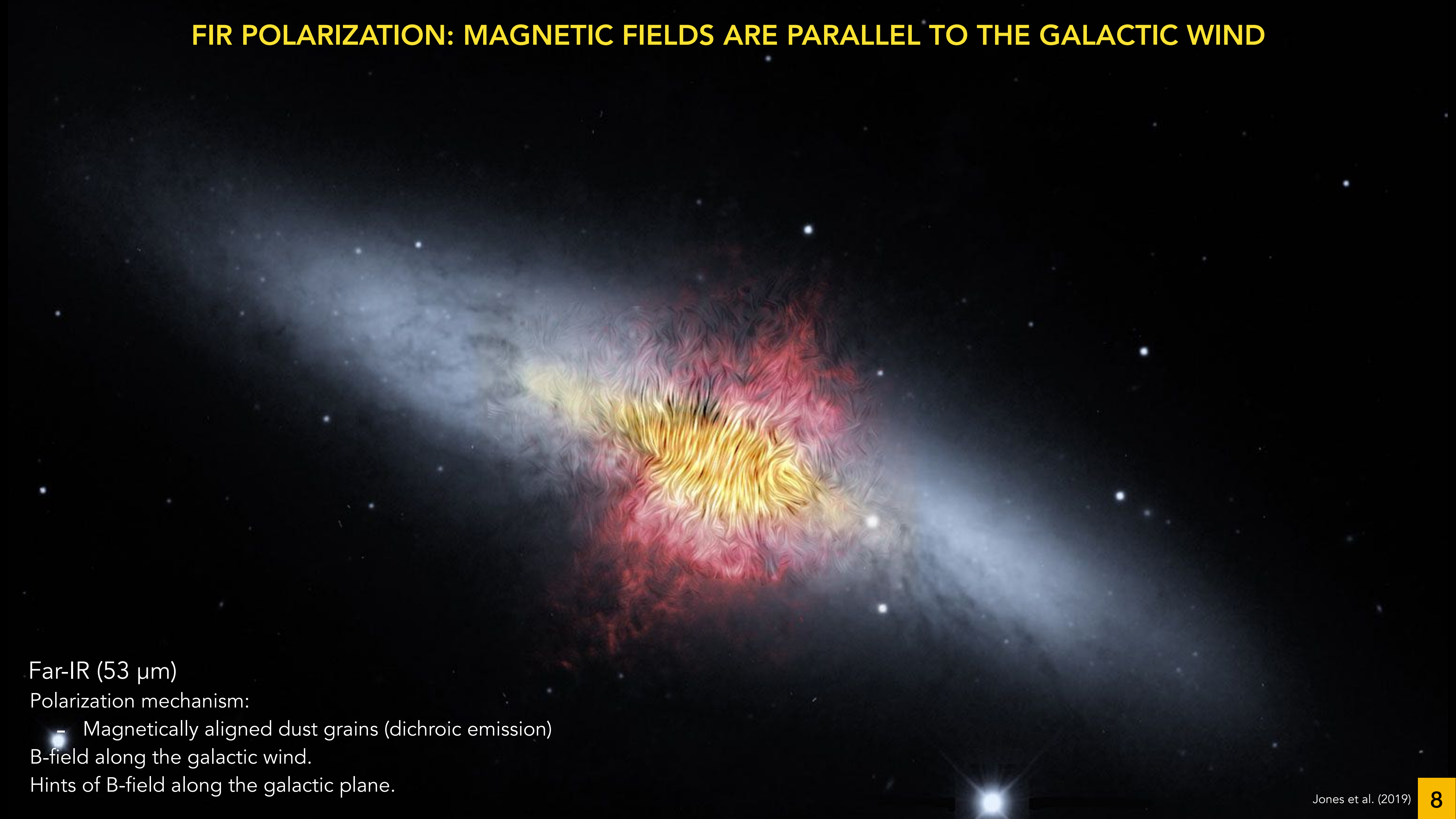
Mathews et al. (2009)

Polarization dominated by magnetically aligned dust grains.
Hints of magnetic fields along the:

- galactic outflow, and
- galactic plane

colorscale: 850 μ m
 $P > 3\sigma$, DP<4% at 10" resolution.

FIR POLARIZATION: MAGNETIC FIELDS ARE PARALLEL TO THE GALACTIC WIND



Far-IR (53 μm)

Polarization mechanism:

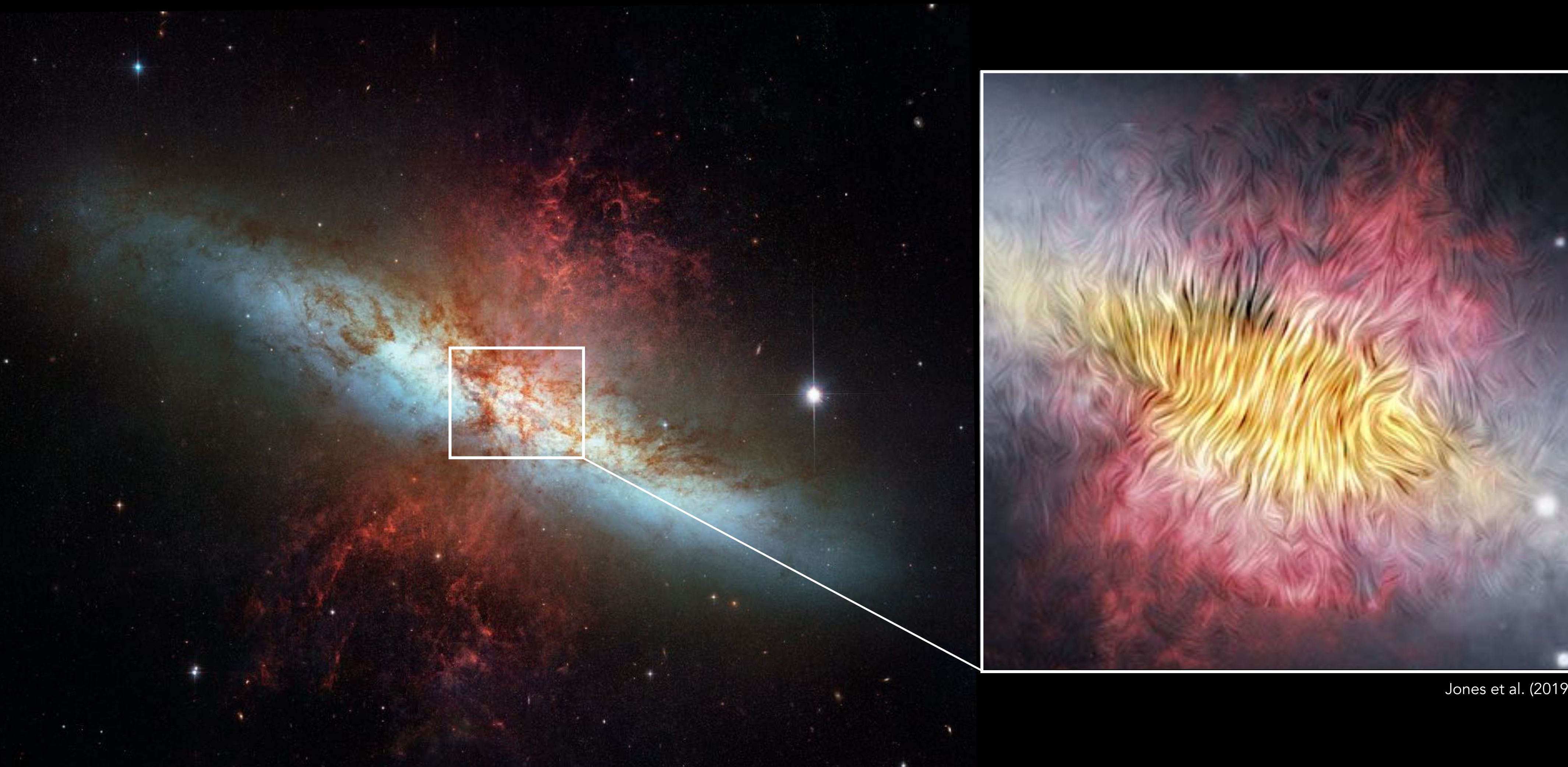
- Magnetically aligned dust grains (dichroic emission)

B-field along the galactic wind.

Hints of B-field along the galactic plane.

SCIENTIFIC MOTIVATION

- What is the energetic balance between B-field and gas kinematics in the wind?
- What does the B-field look like along the galactic wind and in the halo?
- Is the B-field 'open' (galactic outflow) or 'closed' (galactic fountain)?



Jones et al. (2019)

THE DAVIS-CHANDRASEKHAR-FERMI (DCF) METHOD

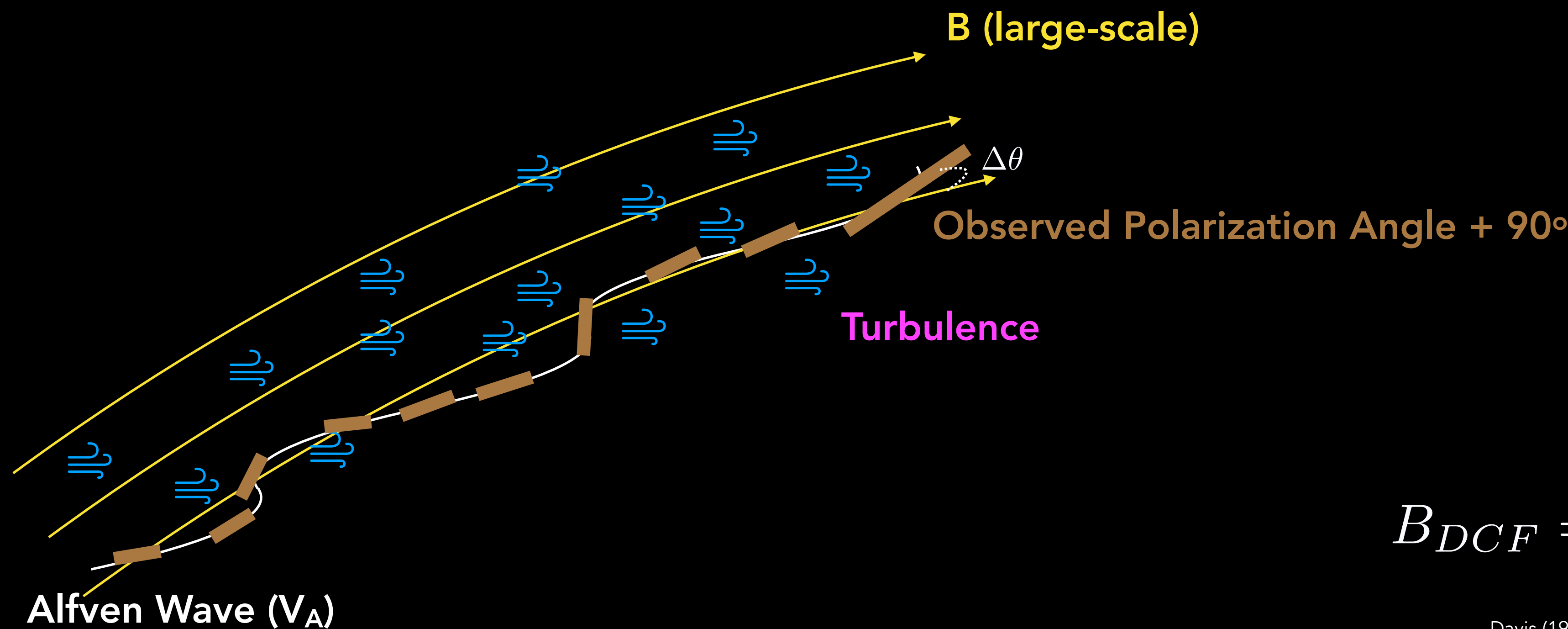
This method assumes:

- Isotropic turbulent medium in all directions.

For a steady-state with no large-scale flows, the Alfvén wave (V_A , velocity of a transverse magnetohydrodynamical wave) is related to the observed dispersion of polarization angles.

We obtain:

- Magnetic field strength in the plane-of-the-sky.



$$B_{DCF} = \xi \sqrt{4\pi\rho} \frac{\sigma_v}{\sigma_\phi}$$

Davis (1951), Chandrasekhar & Fermi (1953)
ξ factor: Ostriker et al. (2001)

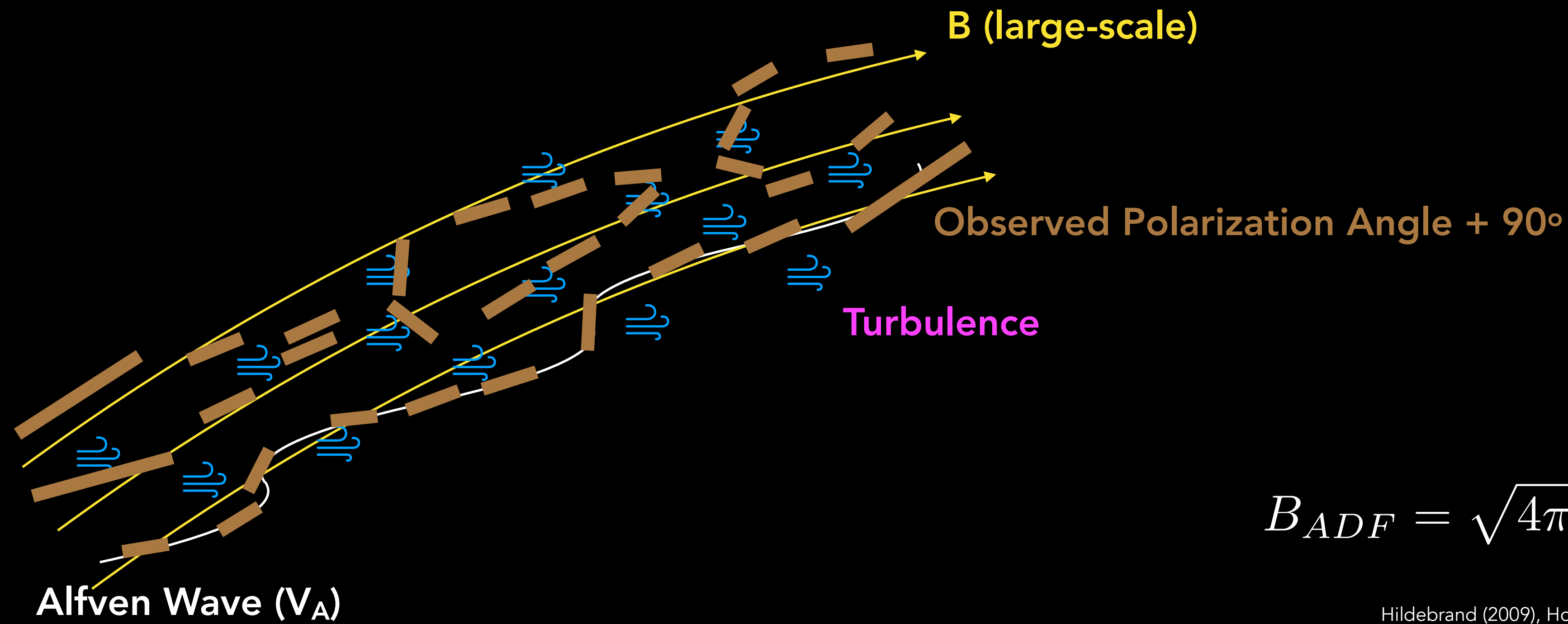
THE DCF METHOD + ANGULAR DISPERSION FUNCTION

This method assumes:

- B-field is a composition of large-scale and turbulent components.
- Two-point structure function (i.e. dispersion function) to describe the angular dispersion as a function of angular scale.

We obtain:

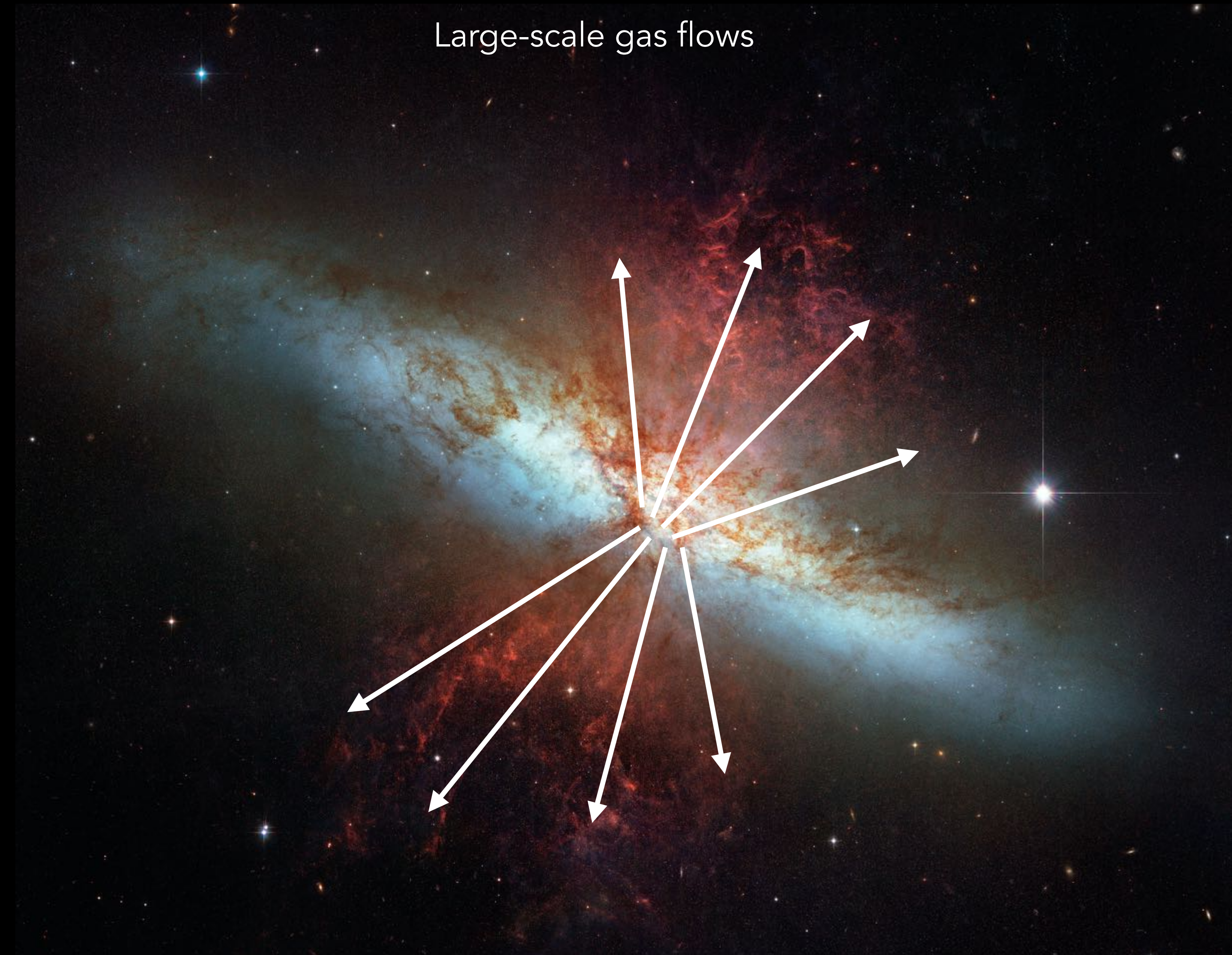
- Turbulence-to-large-scale magnetic energies: $\frac{\langle B_t^2 \rangle}{\langle B_o^2 \rangle}$
- B-field strength of the turbulent component in the plane-of-the-sky.



$$B_{ADF} = \sqrt{4\pi\rho\sigma_v} \left[\frac{\langle B_t^2 \rangle}{\langle B_o^2 \rangle} \right]^{-1/2}$$

Hildebrand (2009), Houde et al. (2009, 2011)

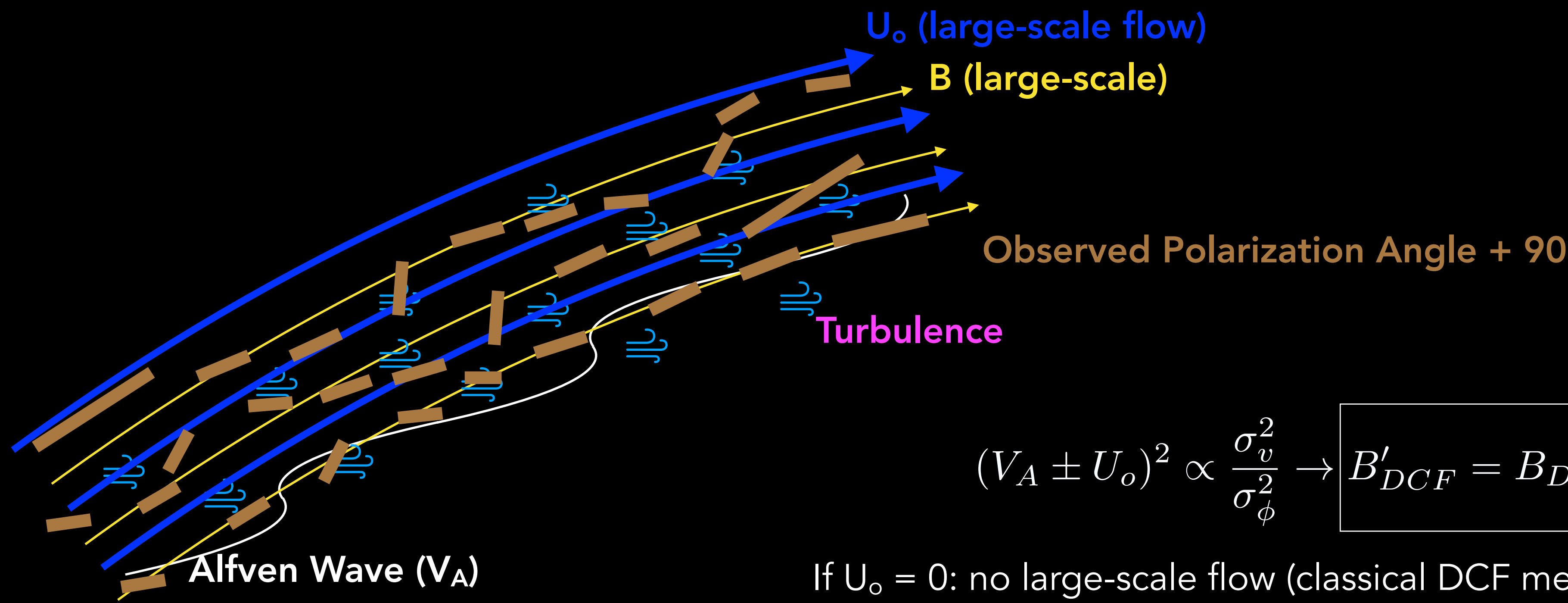
BUT... WE HAVE A BIG PROBLEM USING THE DCF METHOD IN M82



THE EFFECT OF GALACTIC OUTFLOWS IN THE DCF METHOD

This method assumes:

- Steady large-flow in the same direction as the magnetic field orientation.
- Two waves ($V_A + U_o$ and $V_A - U_o$) can satisfy the wave equation.
- FIR polarimetric observations have a 180° ambiguity, no direction is estimated, only orientation.



$$(V_A \pm U_o)^2 \propto \frac{\sigma_v^2}{\sigma_\phi^2} \rightarrow B'_{DCF} = B_{DCF} \left| 1 - \sigma_\phi \frac{U_o}{\sigma_v} \right|$$

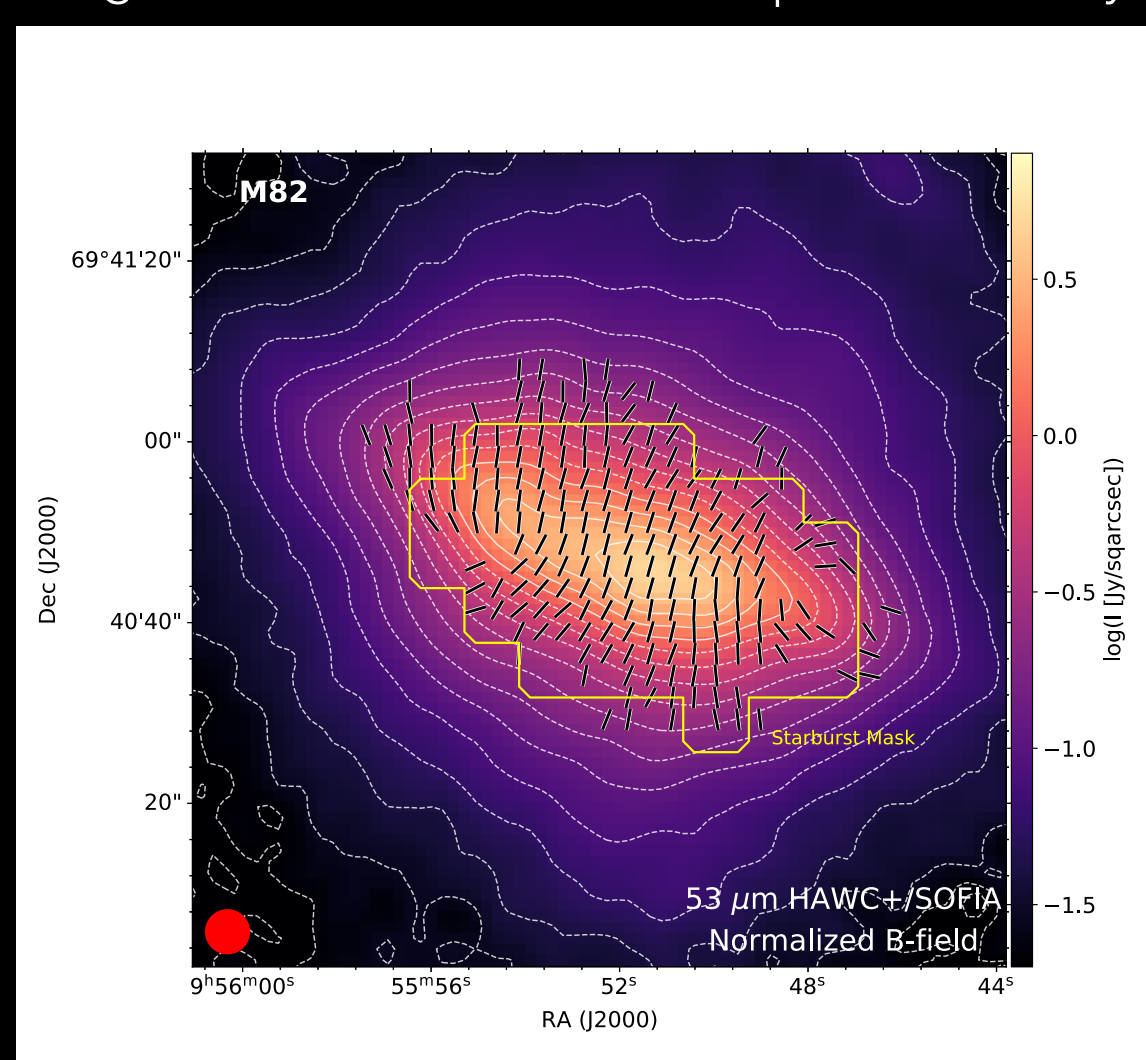
If $U_o = 0$: no large-scale flow (classical DCF method)

If large-scale flow dominates $\rightarrow B_{DCF}$ overestimates the B-field strength

If turbulence dominates $\rightarrow B_{DCF}$ underestimates the B-field strength

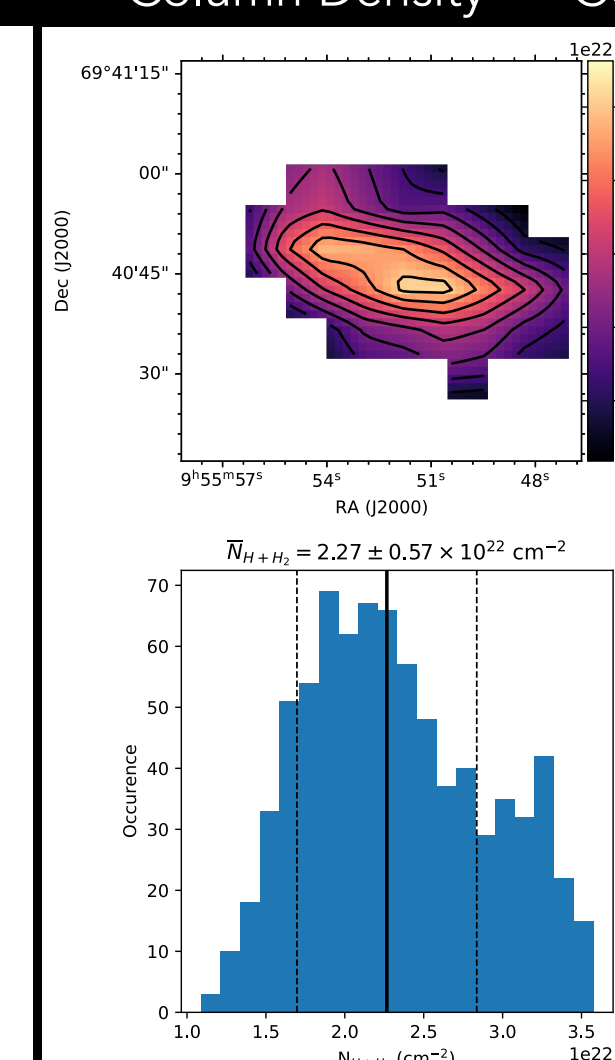
THE DCF METHOD APPLIED TO M82

Magnetic field orientation in the plane of the sky



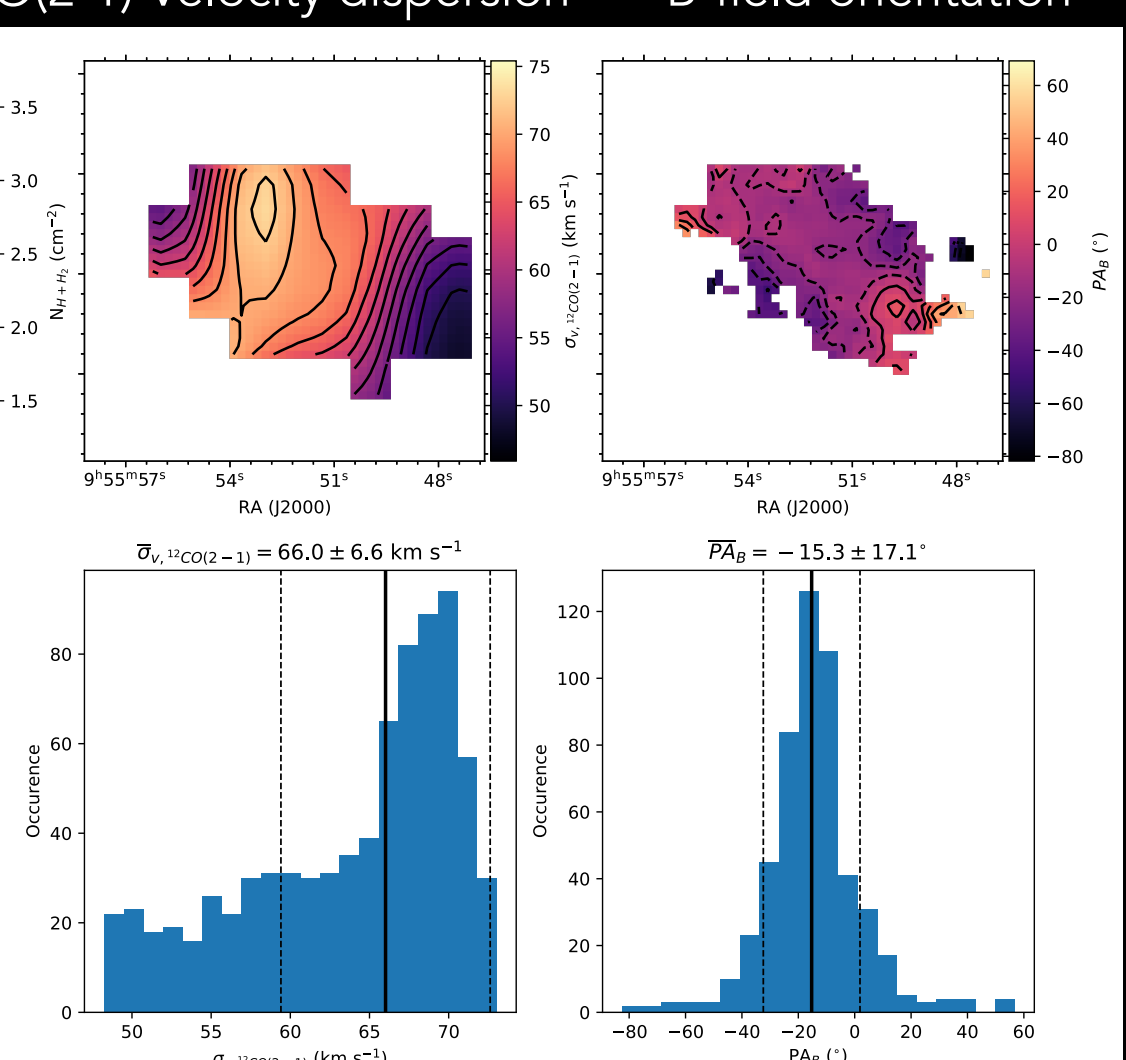
Jones et al. (2019), Contursi et al. (2013)

Column Density



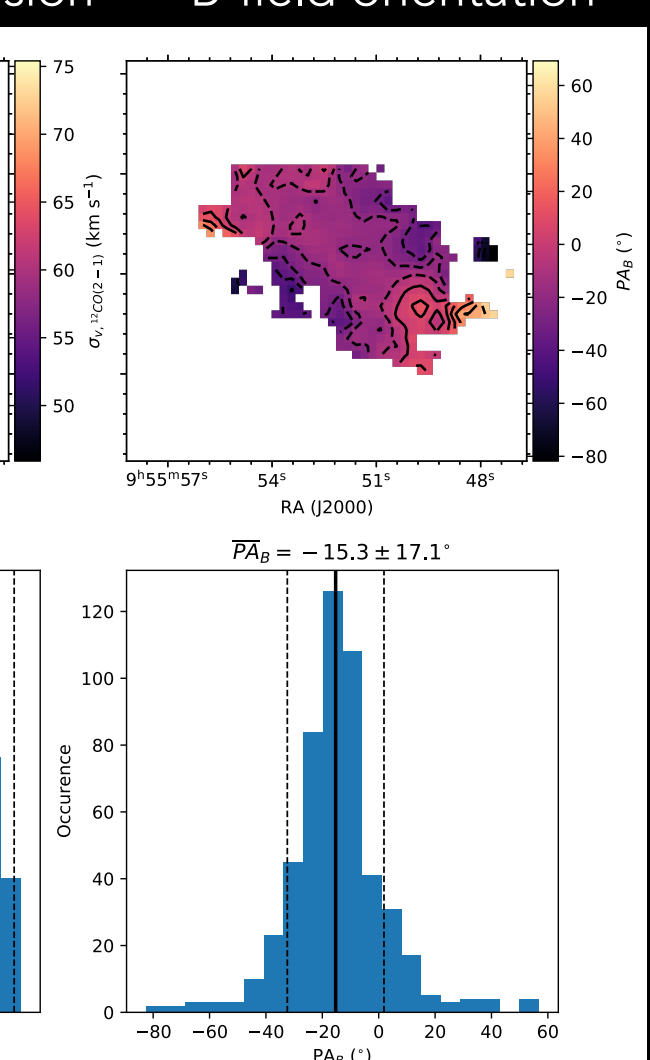
Jones et al. (2019)

CO(2-1) Velocity dispersion



Jones et al. (2019)

B-field orientation



Jones et al. (2019)

Mass Density (ρ)

$$\text{Angular Dispersion} \left[\frac{\langle B_t^2 \rangle}{\langle B_0^2 \rangle} \right]$$

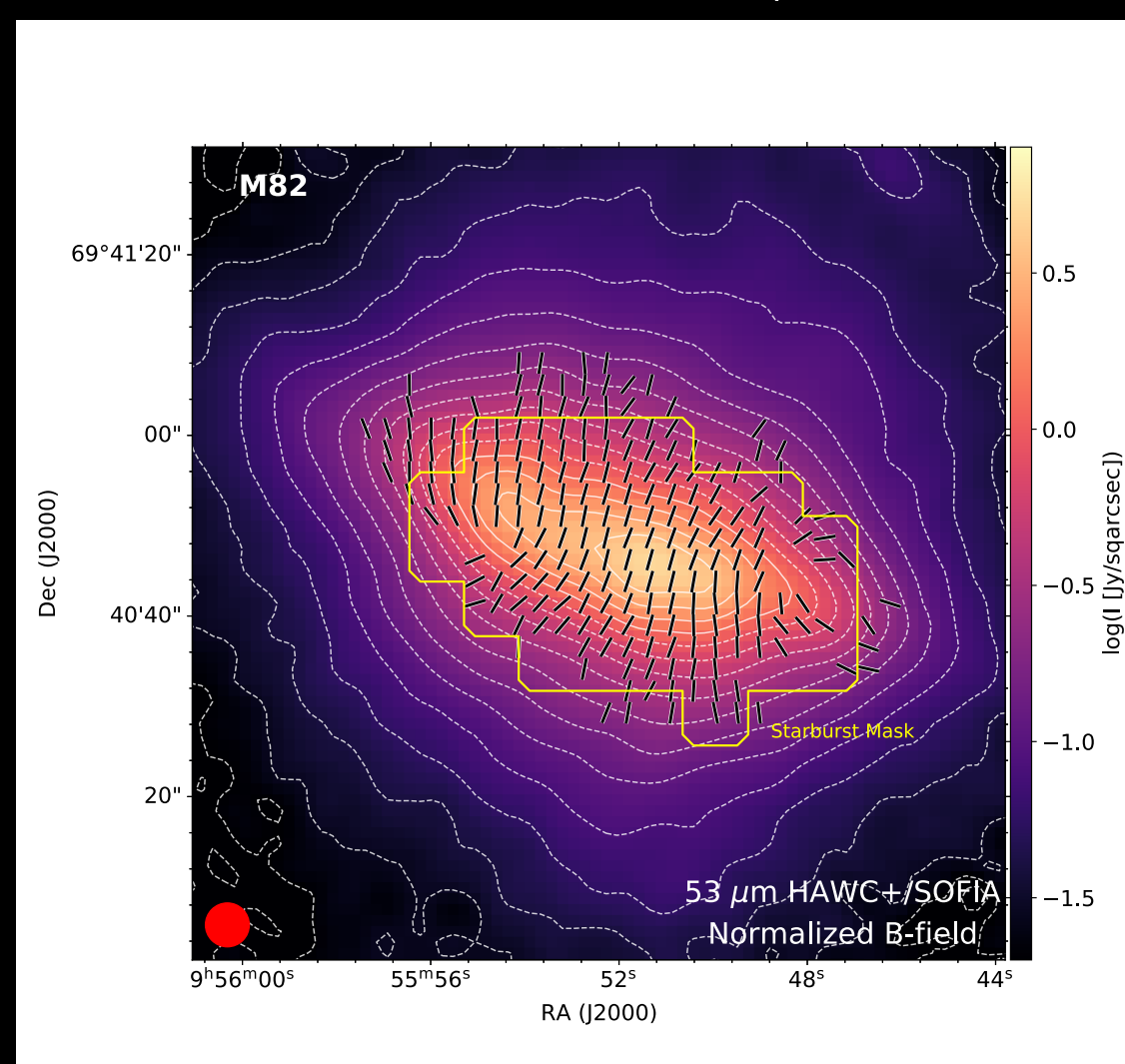
Velocity Dispersion (σ_v)

$$B_{ADF} = \sqrt{4\pi\rho\sigma_v} \left[\frac{\langle B_t^2 \rangle}{\langle B_0^2 \rangle} \right]^{-1/2}$$

$$B_{ADF} = 1.04 \pm 0.17 \text{ mG}$$

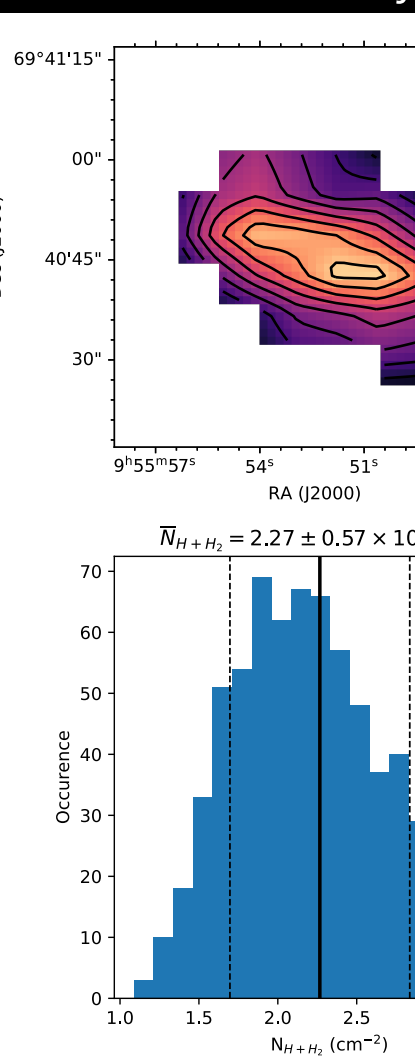
THE DCF METHOD APPLIED TO M82

Magnetic field orientation in the plane of the sky



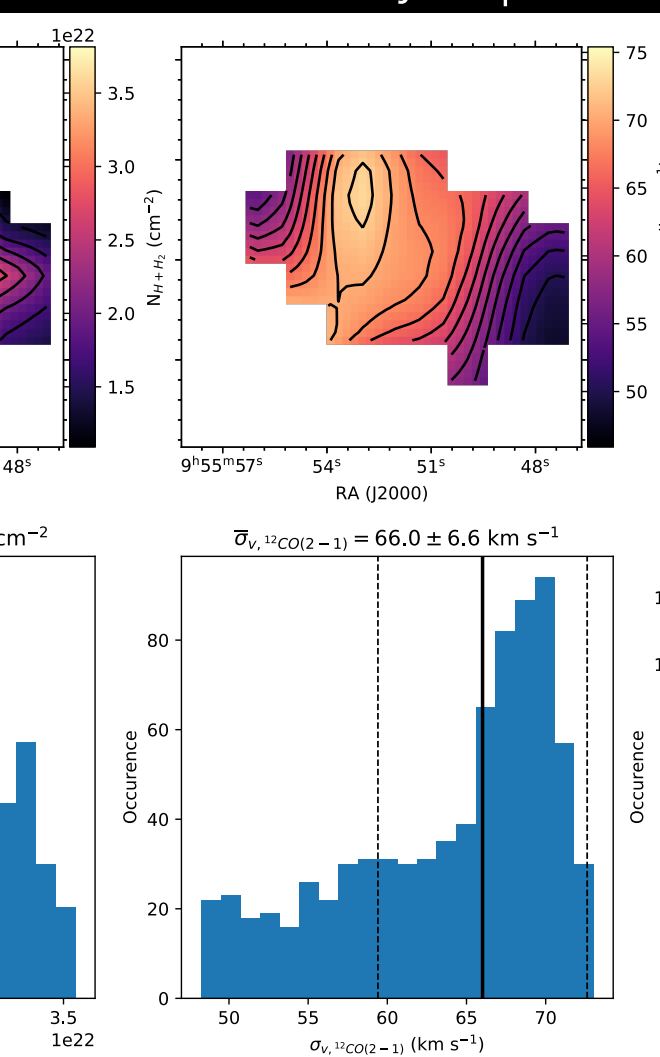
Jones et al. (2019), Contursi et al. (2013)

Column Density



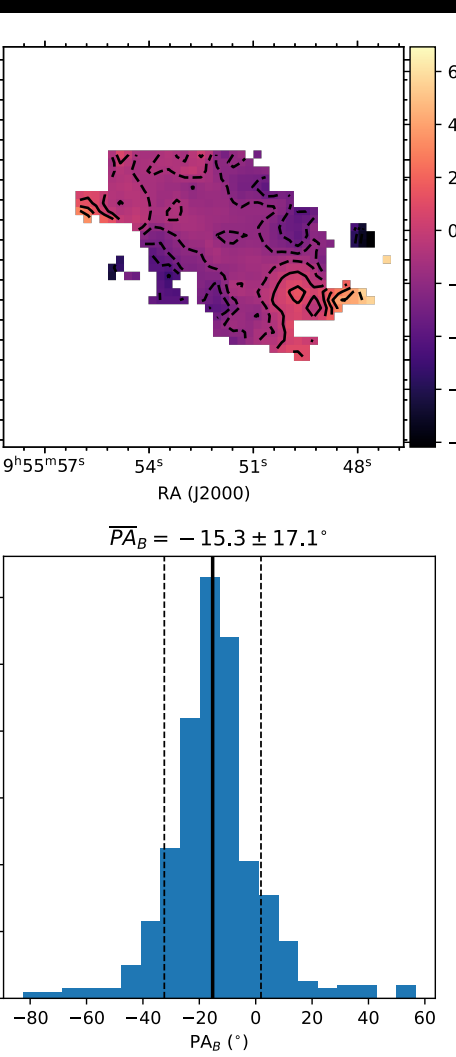
Jones et al. (2019)

CO(2-1) Velocity dispersion



Jones et al. (2019)

B-field orientation



Jones et al. (2019)

Mass Density (ρ)

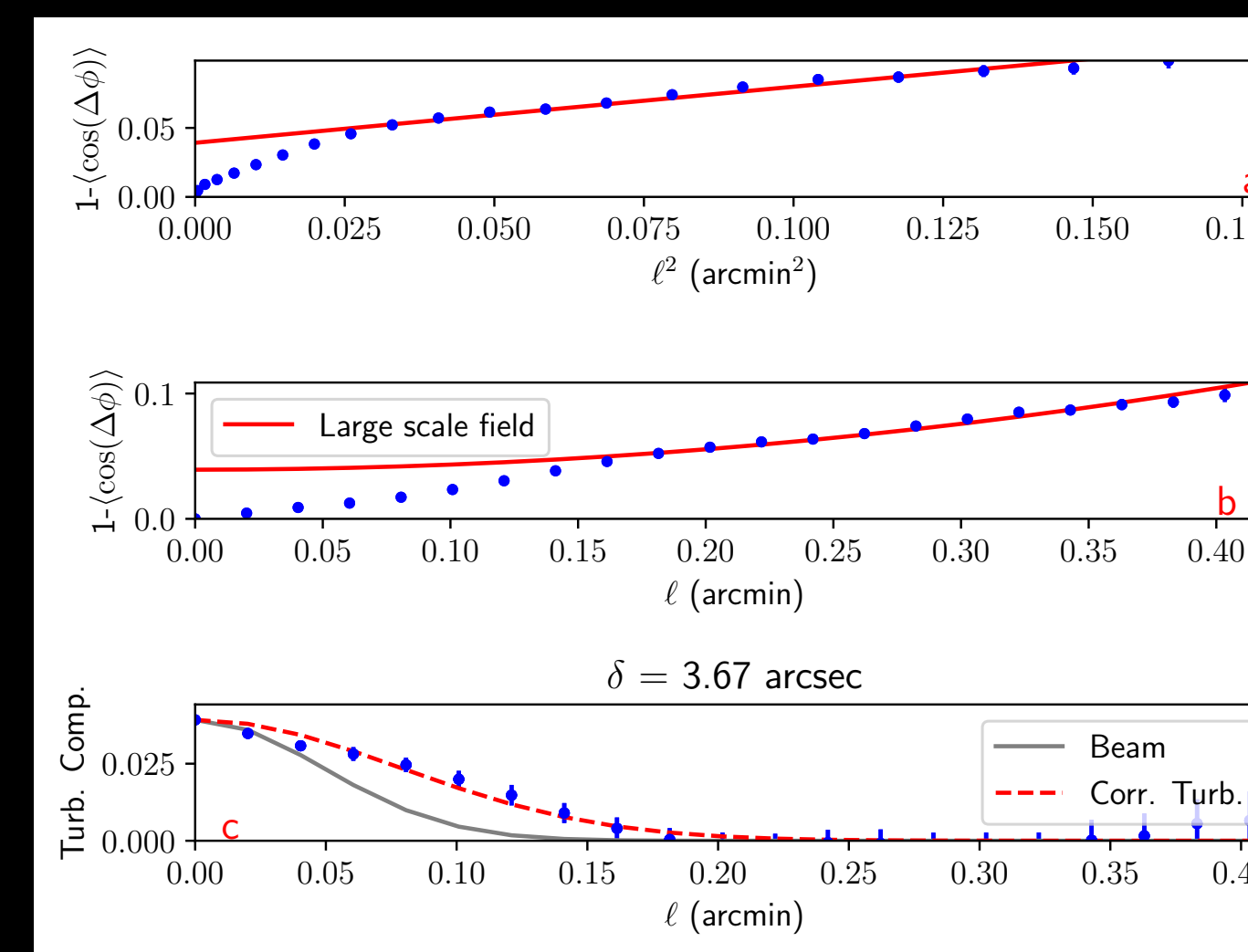
$$\text{Angular Dispersion} \left[\frac{\langle B_t^2 \rangle}{\langle B_0^2 \rangle} \right]$$

Velocity Dispersion (σ_v)

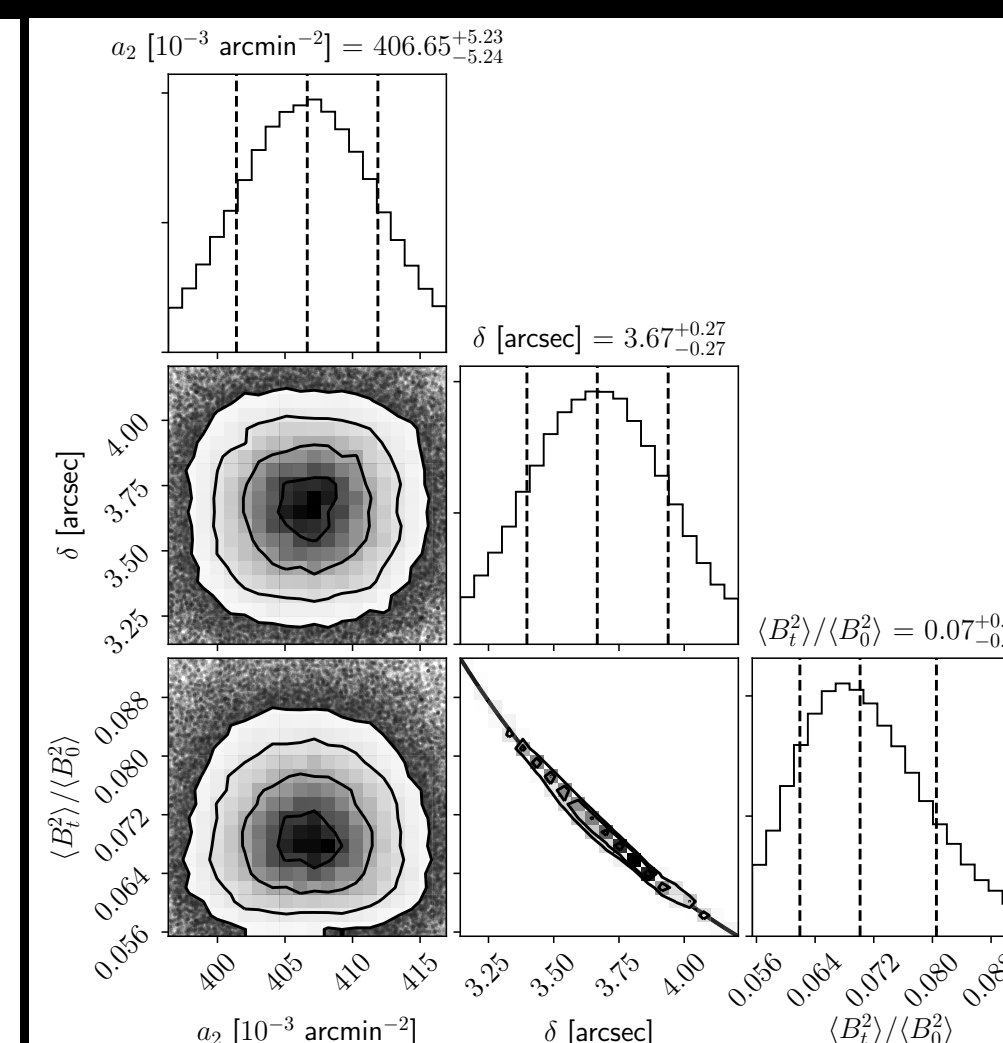
$$B_{ADF} = \sqrt{4\pi\rho\sigma_v} \left[\frac{\langle B_t^2 \rangle}{\langle B_0^2 \rangle} \right]^{-1/2}$$

$$B_{ADF} = 1.04 \pm 0.17 \text{ mG}$$

Angular dispersion function



Posteriors



Using the angular dispersion function:

- The coherent length of the turbulent B-field

$$\delta = 73.6 \pm 5.6 \text{ pc}$$

Adebahr et al. (2007) estimated a coherent length of ~50 pc

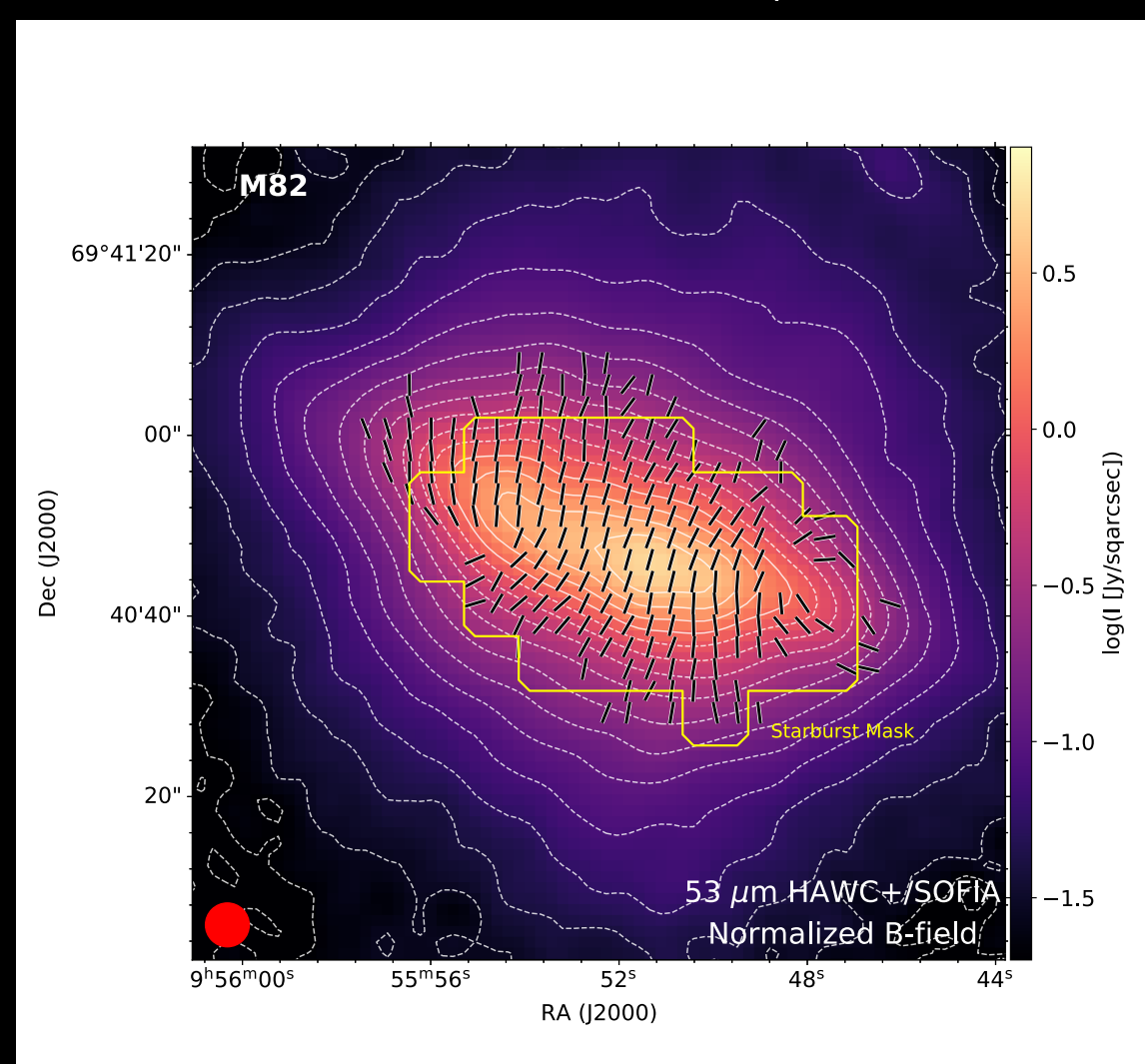
ISM typical turbulence length of 50-100 pc due to SN explosions

is larger than the resolution element of our observations 58 pc.

Turbulence is resolved

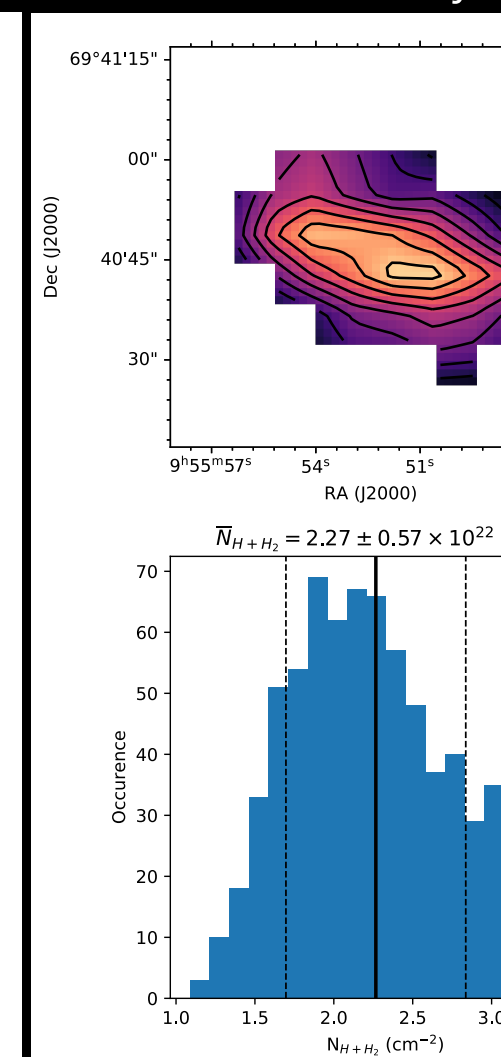
THE DCF METHOD APPLIED TO M82

Magnetic field orientation in the plane of the sky



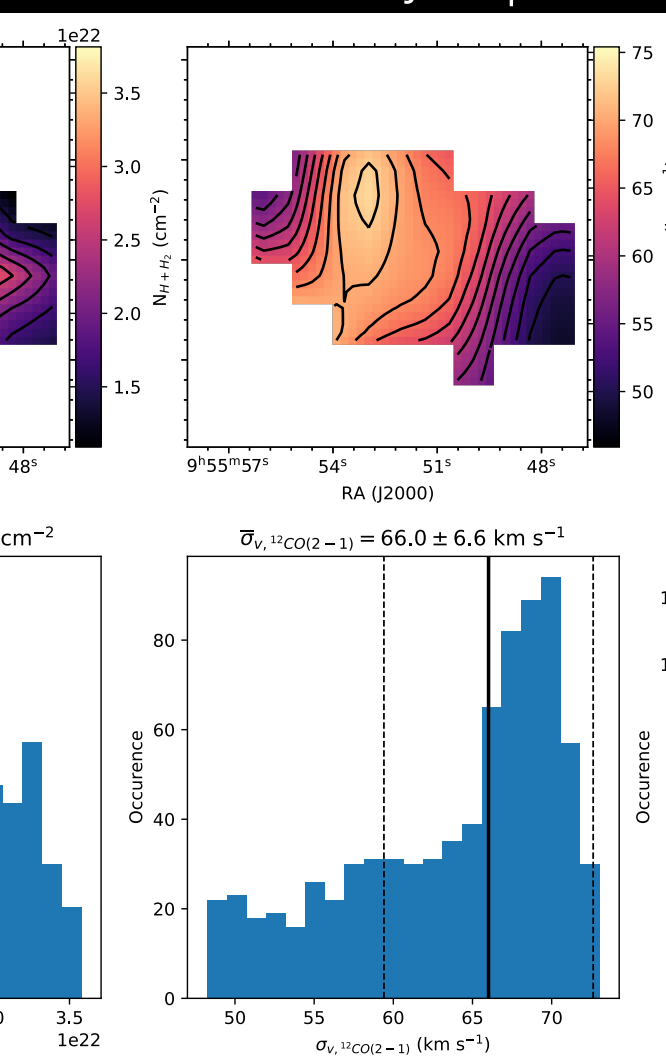
Jones et al. (2019), Contursi et al. (2013)

Column Density



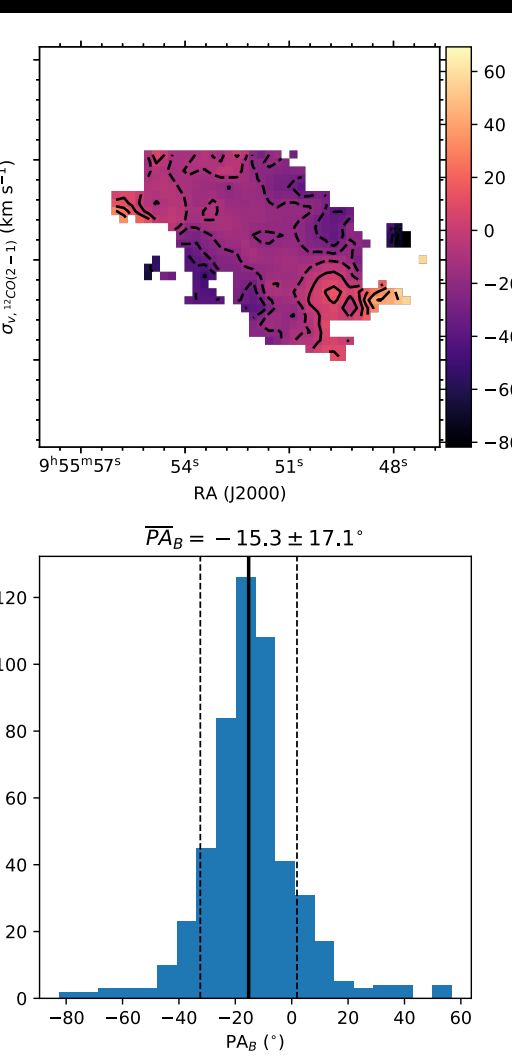
Jones et al. (2019)

CO(2-1) Velocity dispersion



Leroy et al. (2015)

B-field orientation



Jones et al. (2019)

Mass Density (ρ)

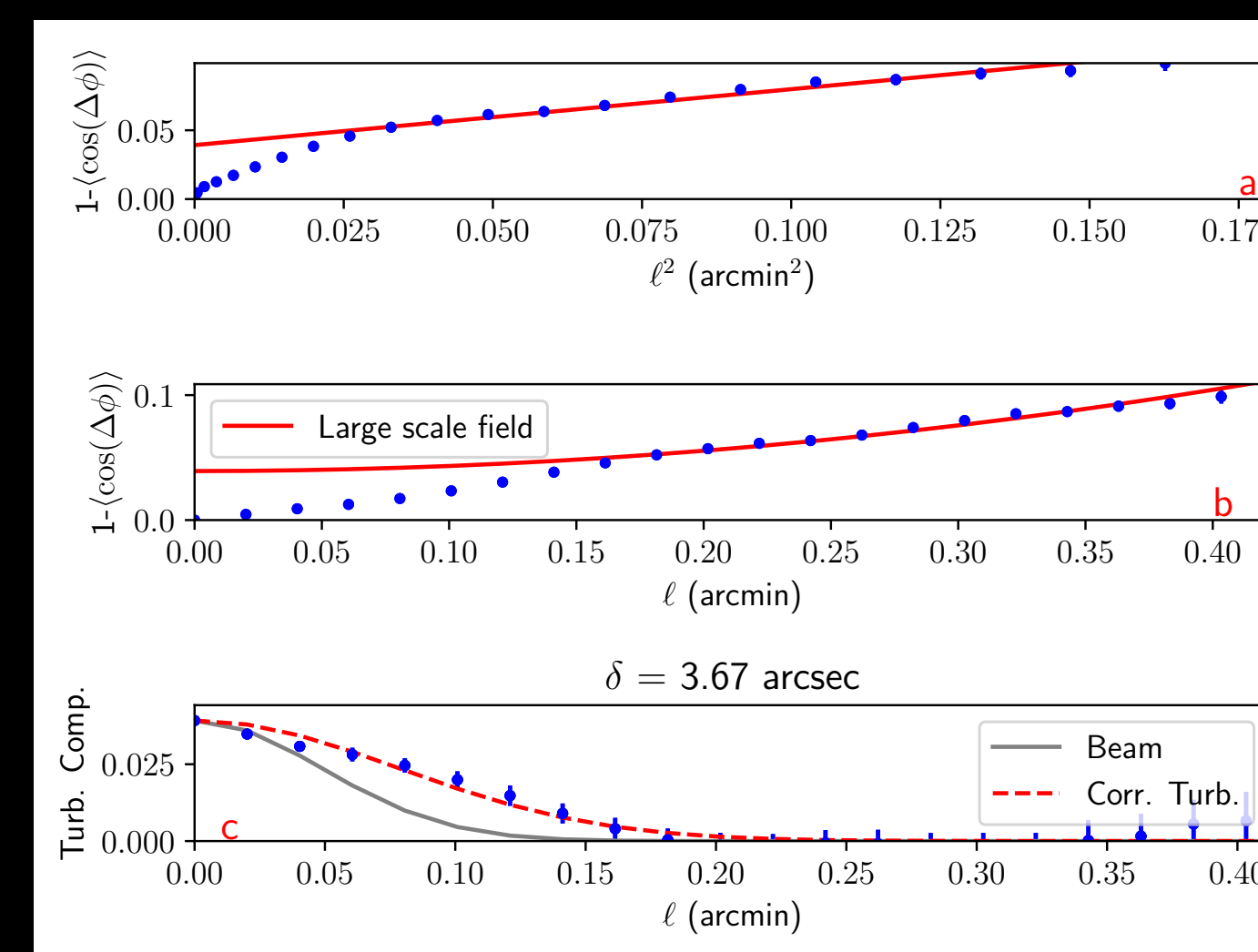
$$\text{Angular Dispersion} \left[\frac{\langle B_t^2 \rangle}{\langle B_0^2 \rangle} \right]$$

Velocity Dispersion (σ_v)

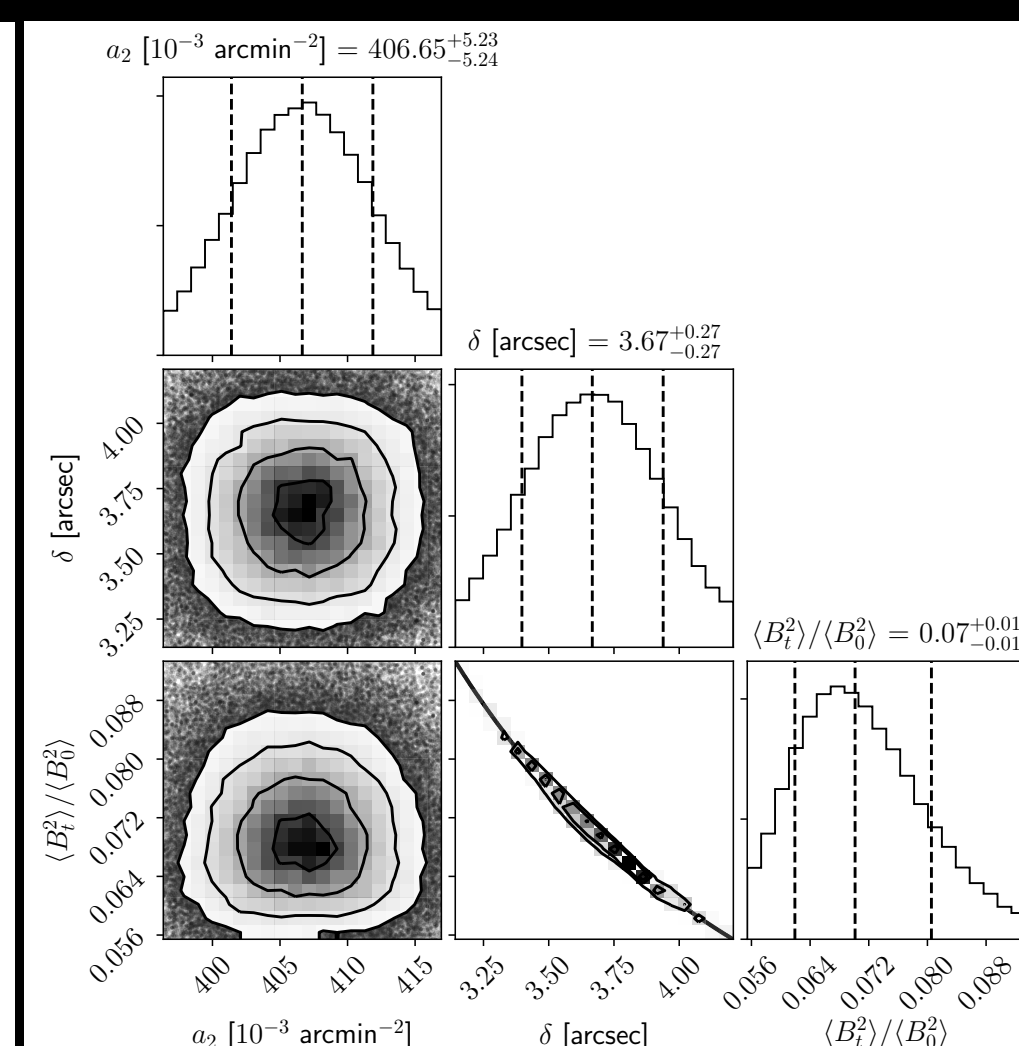
$$B_{ADF} = \sqrt{4\pi\rho\sigma_v} \left[\frac{\langle B_t^2 \rangle}{\langle B_0^2 \rangle} \right]^{-1/2}$$

$$B_{ADF} = 1.04 \pm 0.17 \text{ mG}$$

Angular dispersion function



Posteriors



Large-Scale Flow (U_0)

$$U_0 = 396 \pm 87 \text{ km/s}$$

Leroy et al. (2015)

$$B'_{ADF} = B_{ADF} \left| 1 - \sigma_\phi \frac{U_0}{\sigma_v} \right|$$

Correction of ~25%.

$$B'_{ADF} = 0.77 \pm 0.17 \text{ mG}$$

Mean B-field strength in the starburst mask (873x510 pc²)

~1 mG for the star-forming region, and ~μG weak diffuse component (Adebahr et al. 2007)
~220-240 μG dense core taking into account energy losses (Lacki & Beck 2013)
<1.6 mG using hydrostatic and magnetic equipartition (Thompson et al. 2006)

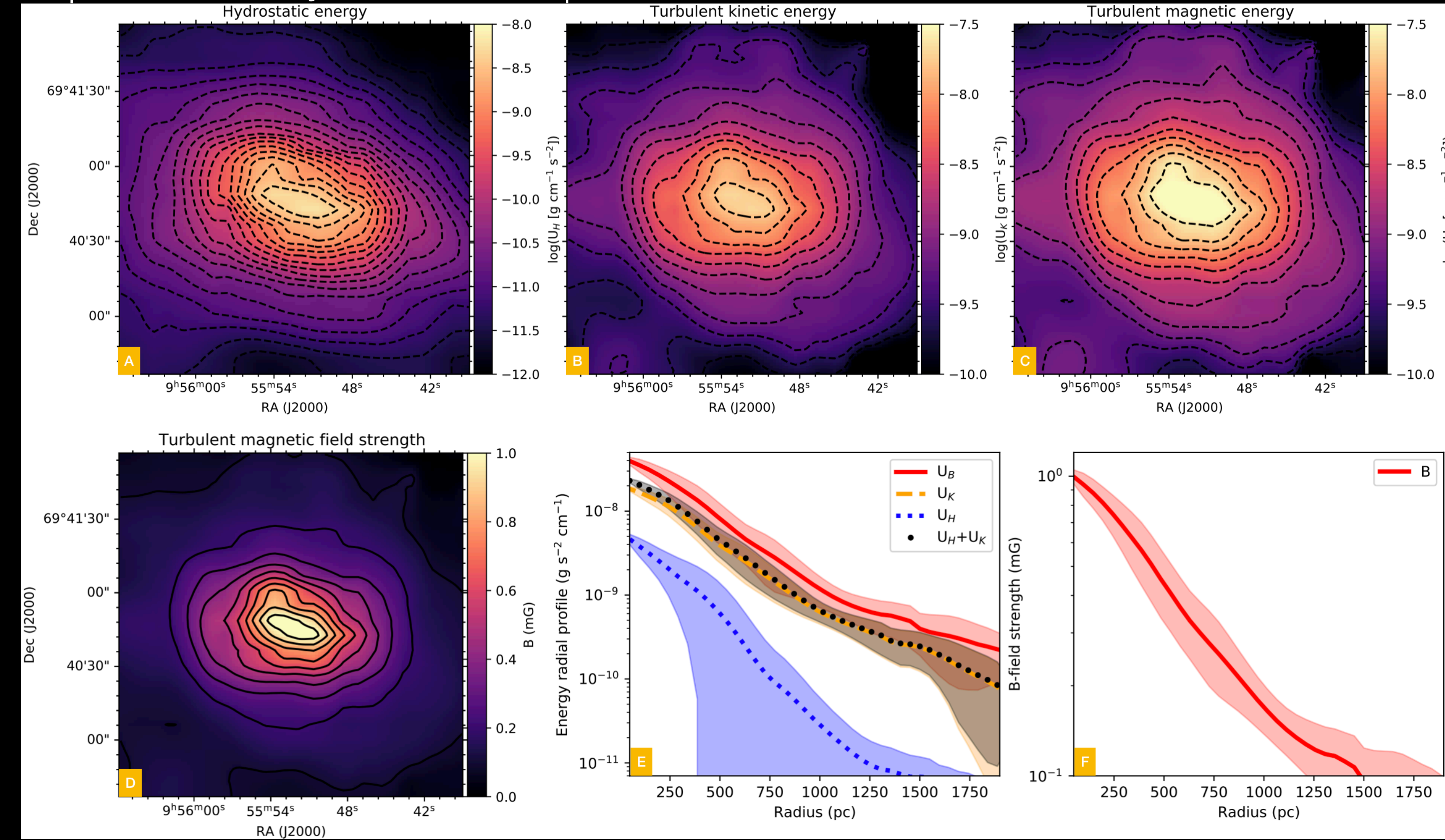
ENERGY BALANCE AND MAP OF THE MAGNETIC FIELD STRENGTH

Energy budget:

- The entrainment between kinetic, thermal, and magnetic energies are defined by the beta parameter: $\beta' = \frac{U_K + U_H}{U_B}$

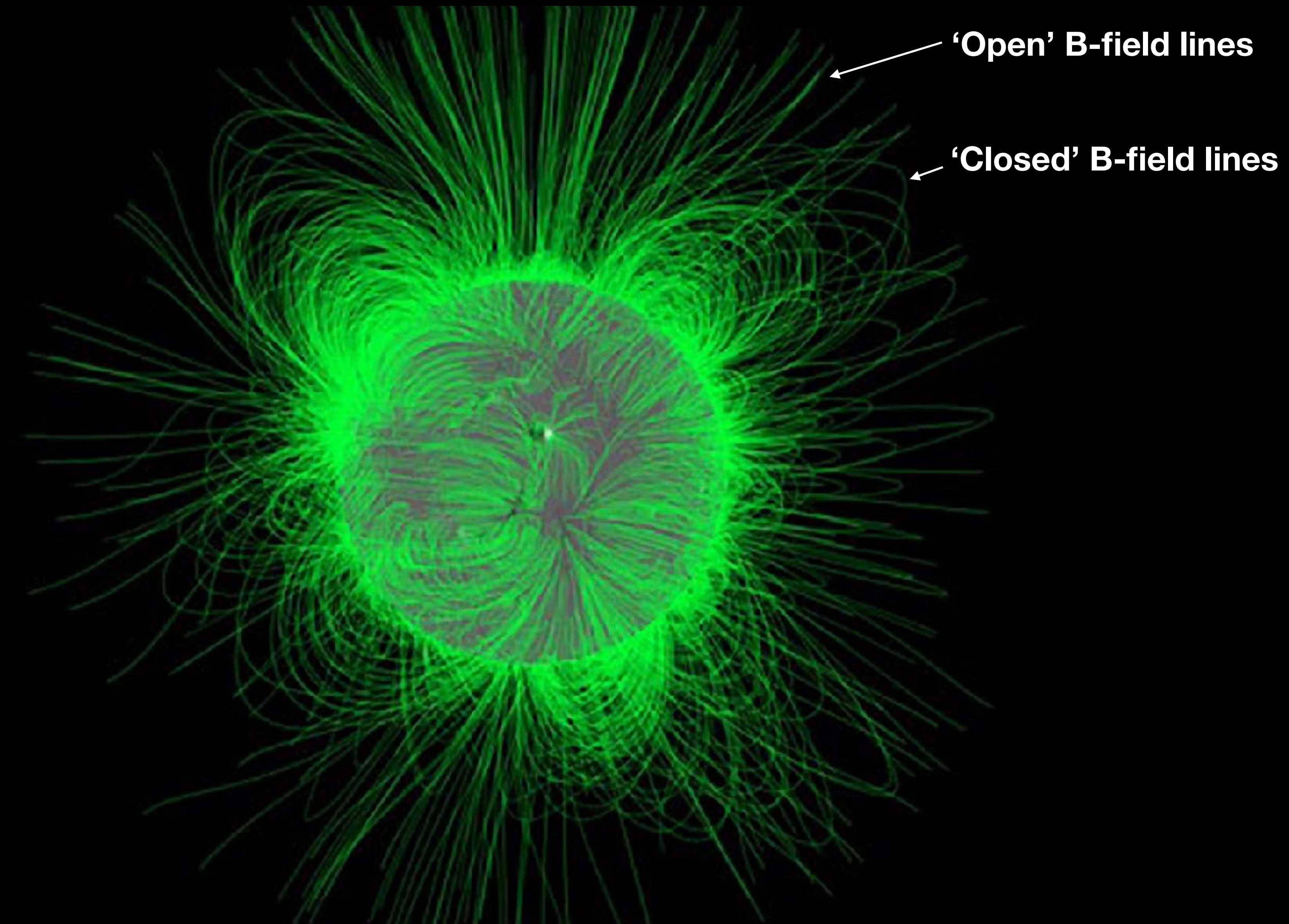
This method assumes:

- Corrected DCF method provides the mean B-field strength within the starburst mask.
- The energy map should satisfy that the beta parameter within the mask $\beta' = 0.56 \pm 0.23$



POTENTIAL FIELD EXTRAPOLATION

The potential field extrapolation is commonly used in solar physics to estimate the B-fields above the corona.

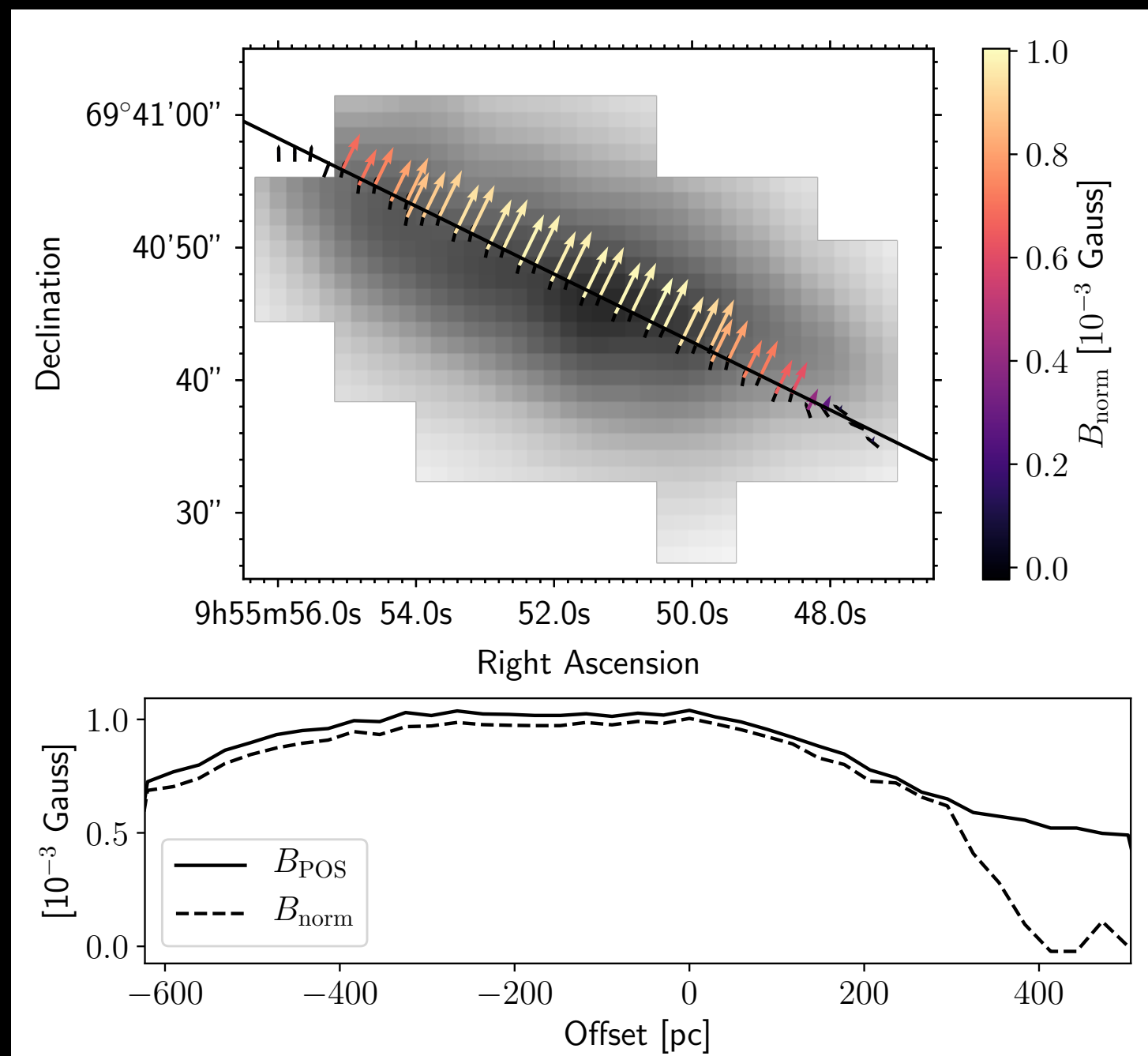


POTENTIAL FIELD EXTRAPOLATION

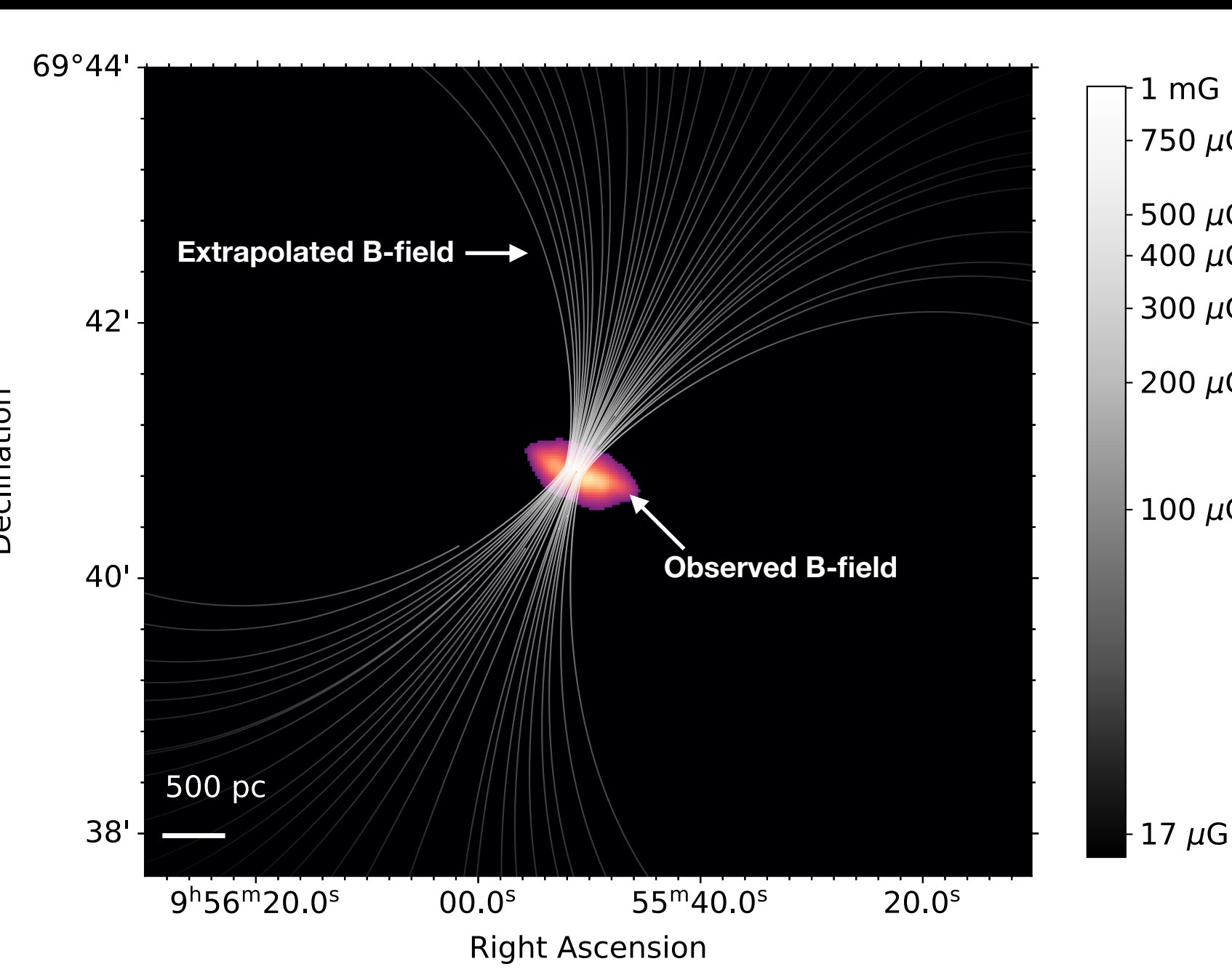
This (very simplified) method:

- Solves the Laplace equation with two boundary conditions:
 1. The B-field strength and orientation in the central plane of the starburst mask.
 2. The B-field strength at infinity is zero.

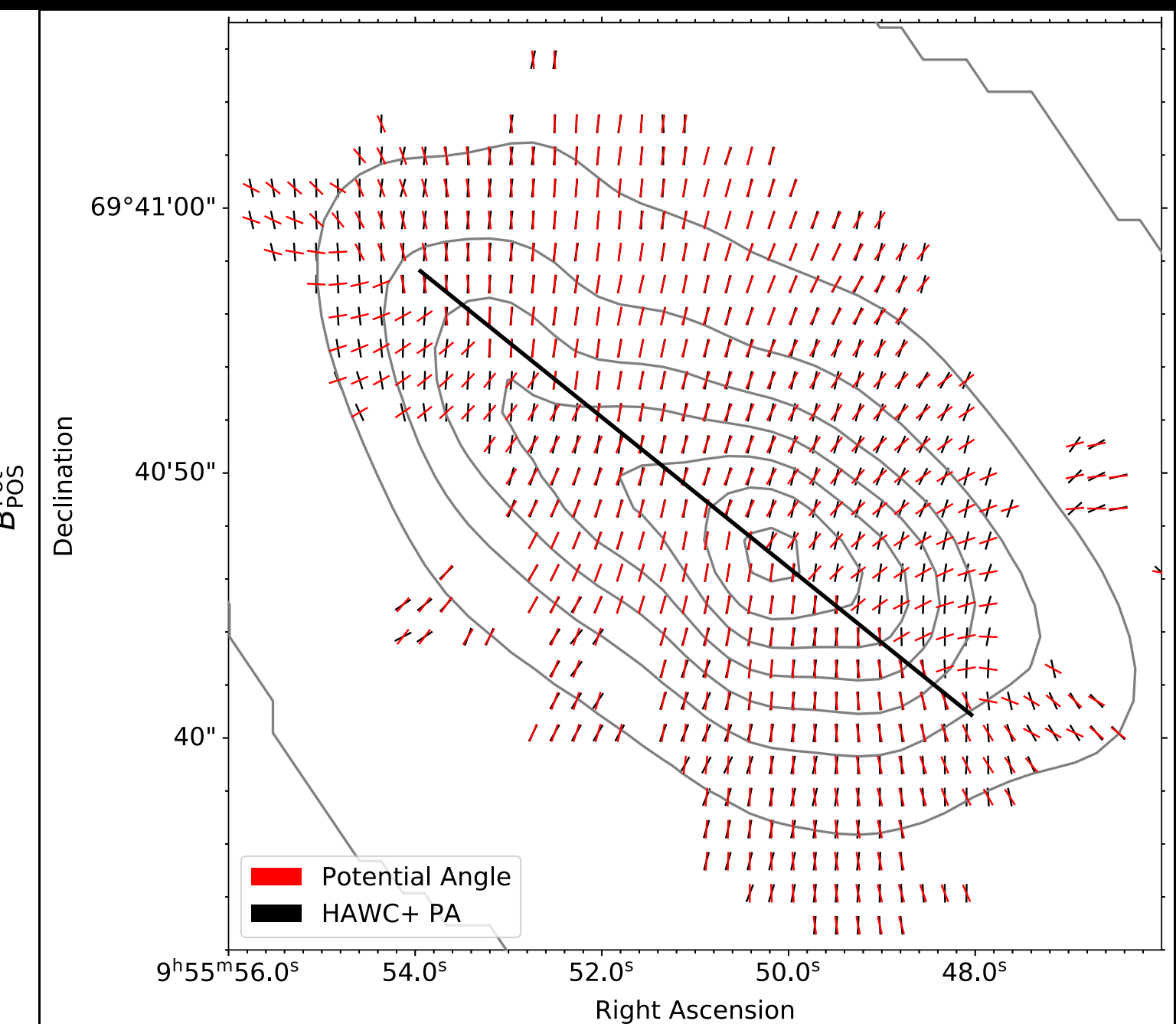
The magnetic field in the central plane of the starburst mask



Extrapolated B-field strength and orientation



Observed vs. extrapolated B-field orientation



MAGNETIC FIELD ALONG THE GALACTIC OUTFLOW

Central 300 pc radius (measured):

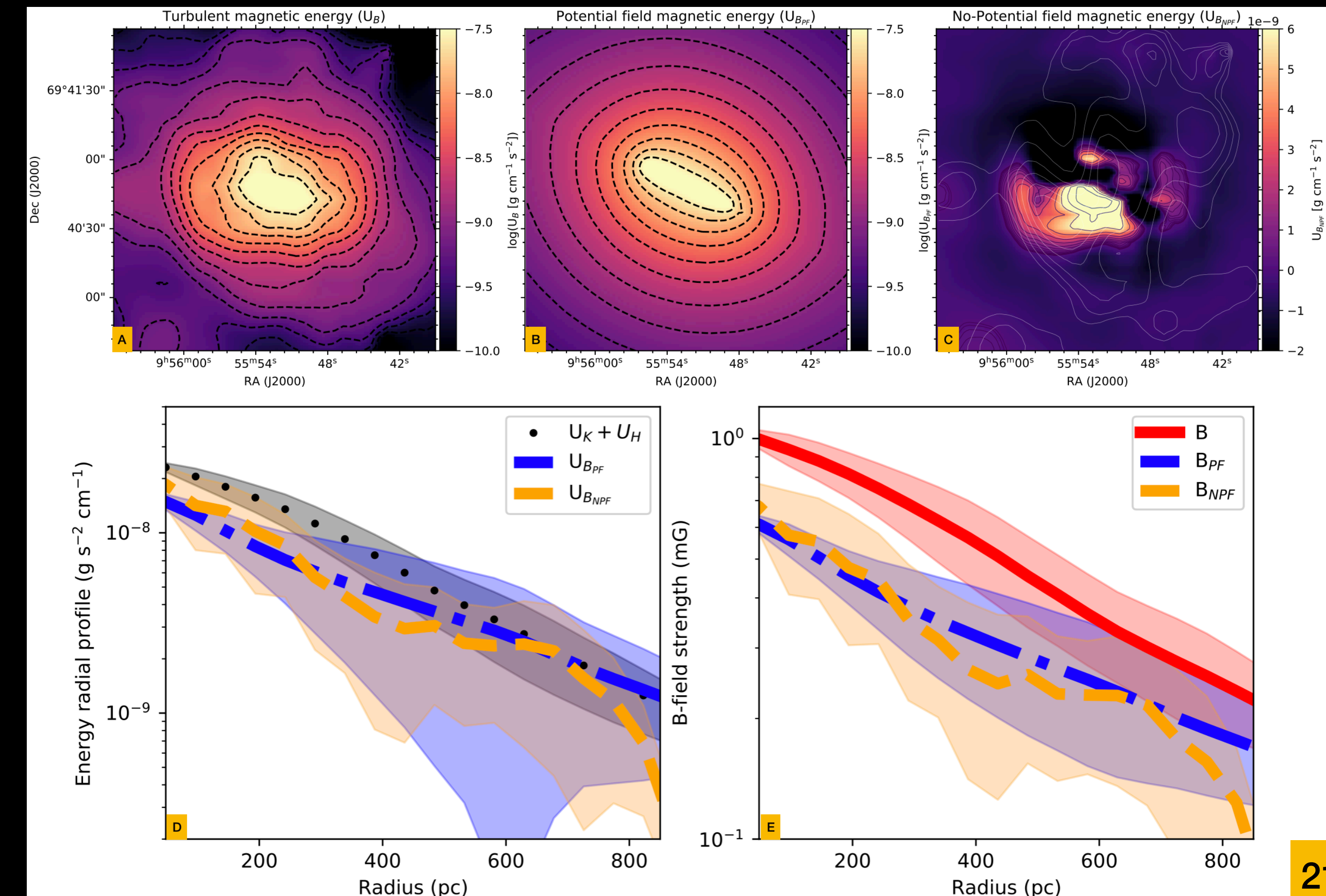
- B-field energy arises from two different physical components:
 1. Large-scale (anisotropic turbulent) B-field associated with the galactic outflow (potential field)
 2. Small-scale turbulent B-field associated with a bow-shock-like pattern (non-potential field)

- Now:

- $U_K \geq U_{BPF}$ and $U_K \geq U_{BNPF} \rightarrow$ The turbulent kinetic energy is slightly larger than each of the individual turbulent magnetic fields within the starburst region.

300 pc > R < 2 kpc (measured):

- Turbulent kinetic and turbulent B-field energies are in close equipartition: $U_K \sim U_{BPF}$.
- No contribution of the small-scale B-field.



MAGNETIC FIELD ALONG THE GALACTIC OUTFLOW

Central 300 pc radius (measured):

- B-field energy arises from two different physical components:
 1. Large-scale (anisotropic turbulent) B-field associated with the galactic outflow (potential field)
 2. Small-scale turbulent B-field associated with a bow-shock-like pattern (non-potential field)
- Now:
 - $U_K \geq U_{BPF}$ and $U_K \geq U_{BNPF} \rightarrow$ The turbulent kinetic energy is slightly larger than each of the individual turbulent magnetic fields within the starburst region.

300 pc > R < 2 kpc (measured):

- Turbulent kinetic and turbulent B-field energies are in close equipartition: $U_K \sim U_{BPF}$.
- No contribution of the small-scale B-field.

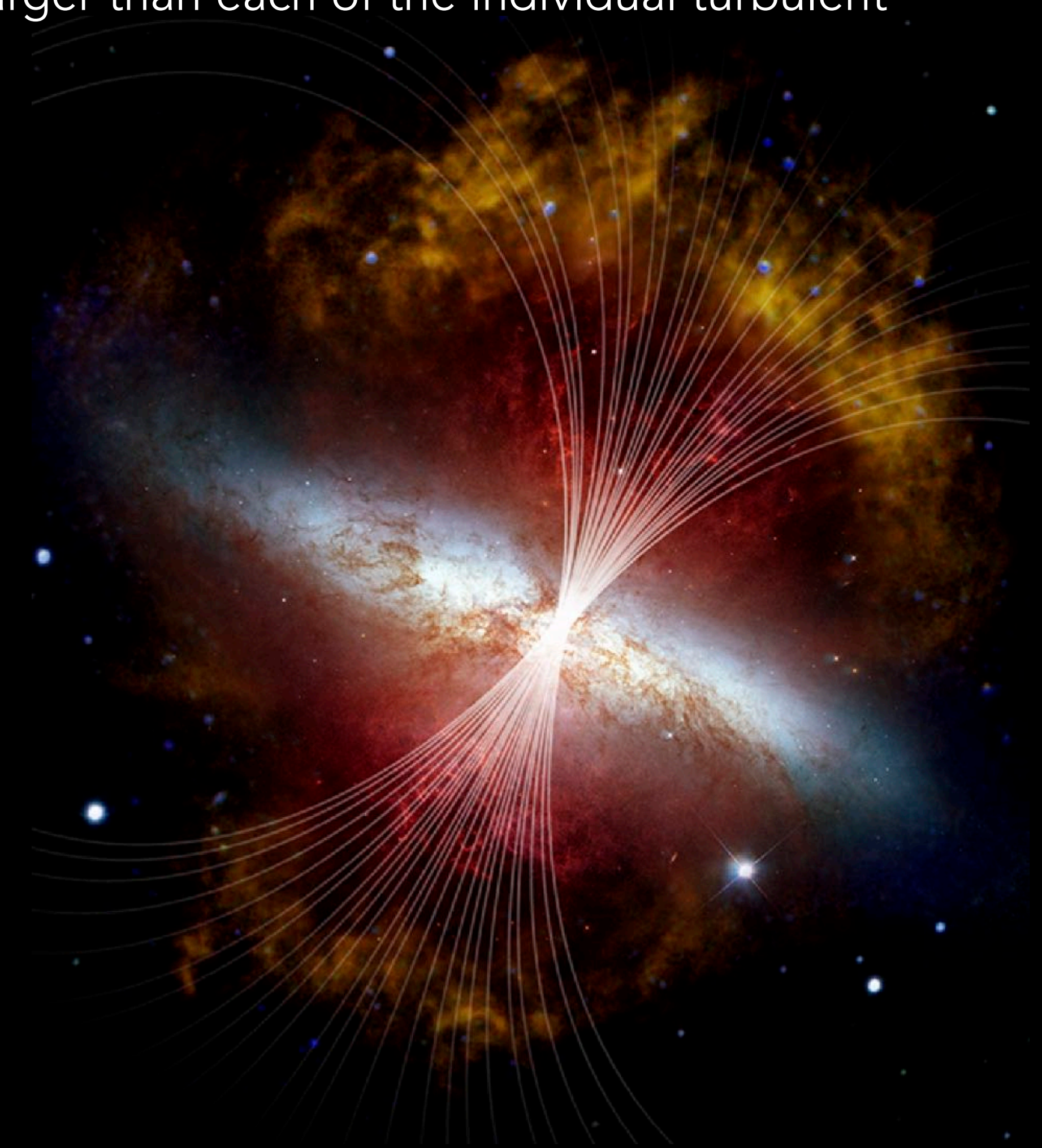
R ~ 6.6 kpc (extrapolated):

- U_K (clouds) > U_{BPF}
- U_K (ambient) << U_{BPF}

Magnetic fields are 'open'

Material scapes to the circumnuclear galactic medium driven away by the kinetic energy of the galactic outflow.

Galactic Outflow





A NEW ERA OF MEASURING MAGNETIC FIELDS IN GALAXIES WITH SOFIA

SOFIA LEGACY PROGRAM

ENRIQUE LOPEZ-RODRIGUEZ
KIPAC/Stanford

ANN SUI MAO
Max-Planck, Bonn

<http://galmagfields.com/>